

[Click here to view linked References](#)

1 Transcriptome analysis and postharvest behavior of the 2 kiwifruit '*Actinidia deliciosa*' reveal the role of ethylene- 3 related phytohormones during fruit ripening

4
5 Juan Salazar¹, Patricio Zapata², Claudia Silva³, Makarena González⁴, Igor Pacheco³,
6 Macarena Bastías⁵, Claudio Meneses⁵, Claudia Jorquera², Israel Moreno⁶, Paulina
7 Shinya², Rodrigo Infante²

8
9 ¹ Department of Plant Breeding, CEBAS-CSIC, PO Box 164, E-30100 Espinardo,
10 Murcia, Spain

11 ² Departamento de Producción Agrícola, Universidad de Chile, Santa Rosa 11315,
12 Santiago, Chile

13 ³ Instituto de Nutrición y Tecnología de los Alimentos, Universidad de Chile, El Líbano
14 5524, Santiago, Chile

15 ⁴ Departamento de Biología, Universidad de Santiago, Alameda Libertador Bernardo
16 O'Higgins 3363, Santiago, Chile

17 ⁵ Centro de Biotecnología Vegetal, Universidad Andrés Bello, Avenida República 330,
18 Santiago, Chile

19 ⁶ Departamento de Ingeniería Química, Universidad de Santiago, Alameda Libertador
20 Bernardo O'Higgins, 3363 Santiago, Chile

21
22 ✉ e-mail: jasalazar@cebas.csic.es

23 Phone number: 0034 968 396 295

24 25 Abstract

26 Kiwifruit are climacteric fruit, so they must be harvested before they are fully ripe,
27 allowing for the extension of their shelf-life via cold storage. Therefore, an adequate
28 knowledge about how ethylene-induced fruit senescence is required to avoid significant
29 economic losses. The main goal of the present study was to investigate the kiwifruit
30 ripening process at the physiological and molecular levels by RNA-seq after 1-MCP
31 (ethylene inhibitor) and Ethrel® (ethylene stimulator) treatments. The results showed that
32 Ethrel® (ethephon) treatment induced more accelerated fruit ripening, leading to rapid
33 fruit senescence, meanwhile 1-MCP (1-Methylcyclopropene) caused a slowing flesh
34 softening, and thus a longer shelf-life period. The RNA-seq was carried out on the fruit
35 after 4 and 13 days, considering day 4 as the most determinant in terms of differentially

1
2
3
4
5
6
7
8
9
10
11
12
13
14
15
16
17
18
19
20
21
22
23
24
25
26
27
28
29
30
31
32
33
34
35
36
37
38
39
40
41
42
43
44
45
46
47
48
49
50
51
52
53
54
55
56
57
58
59
60
61
62
63
64
65

expressed genes (DEGs). The sequencing achieved 70.7 % alignment with the ‘Hongyang’ genome, obtaining 18,036 DEGs. The protein-protein interaction (PPI) network shows the interaction between different pathways in two main clusters: (1) pentose and glucuronate interconversions, citrate cycle, glycolysis and gluconeogenesis or starch and sucrose metabolism and (2) porphyrin and chlorophyll metabolism. The first cluster is mainly interconnected by G6PD1 (pentose pathway); E1 ALPHA and ACLB-2 (citrate cycle); Achn209711 (pentose and glucuronate); LOS2 (glycolysis); HKL1 and HXK1 (glycolysis – starch and sucrose); and PHS2 (starch and sucrose). In the second cluster GUN5 through PORA is interacting with CRD1 and NYC1 which were overexpressed by 1-MCP in the porphyrin and chlorophyll metabolism. In addition, genes linked to PSBY and PSBP photosynthesis-linked proteins in photosystem 2 were overexpressed by 1-MCP which is undoubtedly related to chlorophyll degradation and fruit senescence. These results suggest that in kiwifruit the main pathways that are regulated by ethylene-induced senescence comprise sugar catabolism and chlorophyll degradation.

51 **Keywords**

52 *Actinidia deliciosa*, Kiwifruit, Postharvest, Ethylene, 1-MCP, RNA-seq

59 Introduction

1
2
3 60 Kiwifruit belong to the *Actinidia* genus, and due to its sensory and health attributes
4
5 61 is highly appreciated by consumers. Among kiwifruit, *Actinidia chinensis* Planchon, *A.*
6
7 62 *deliciosa* (*A. chinensis* var. *deliciosa* A. Chevalier), *A. arguta* (Siebold and Zuccarini)
8
9 63 Planchon ex Miquel, and *A. eriantha* Bentham are the most widely cultivated species
10
11 64 around the world (Datson & Ferguson, 2011; Huang et al. 2013). However, the hexaploid
12
13 65 ‘Hayward’ variety ($2n = 6x$) is by far the most commercialized green fleshy kiwifruit.
14
15 66 *Actinidia* genera holds different polyploid species with a haploid number of chromosomes
16
17 67 ($x = 29$), among them *A. deliciosa*, a hexaploid ($6n = 174$), and *A. chinensis* ($2n = 58$)
18
19 68 (Atkinson et al. 1997). It has recently been reported that the draft genome sequence of
20
21 69 heterozygous kiwifruit, known as ‘Hong Yang’ (*A. chinensis*), and the assembled genome
22
23 70 have a total length of 616.1 Mbp and contain 39,040 genes (Huang et al. 2013). Therefore,
24
25 71 this first genome is considered an essential reference for researchers, allowing the
26
27 72 scientific community an useful molecular tool for analyzing important postharvest and
28
29 73 fruit quality traits.

30
31
32 74 Kiwifruit is climacteric, meaning that the fruit will continue to ripen after harvest.
33
34 75 Therefore, kiwifruit is harvested when still unripe and is then kept in cold storage for long
35
36 76 periods. Rhodes et al. (1980) defined the climacteric phase as the moment in which fruit
37
38 77 experience biochemical changes, starting with autocatalytic ethylene production. Thus,
39
40 78 the beginning stage of ethylene emission is involved in the changes that initiate the fruit
41
42 79 senescence, which promotes an increase in respiration and flesh softening. Seymour et al.
43
44 80 (1993) and Wills et al. (1998) noted that non-climacteric fruit show a gradual decrease in
45
46 81 respiration, while climacteric fruit exhibit a peak in their respiratory rates. In some cases,
47
48 82 the climacteric phase involves an increase in respiration, thereby increasing ethylene
49
50 83 production. This is the case with both pepper (Tadesse et al. 2002) and kiwifruit (Viera
51
52
53
54
55
56
57
58
59
60
61
62
63
64
65

1
2
3
4
5
6
7
8
9
10
11
12
13
14
15
16
17
18
19
20
21
22
23
24
25
26
27
28
29
30
31
32
33
34
35
36
37
38
39
40
41
42
43
44
45
46
47
48
49
50
51
52
53
54
55
56
57
58
59
60
61
62
63
64
65

84 et al. 2010; Park et al. 2015). Other authors have shown that the major ethylene rise may
85 take place before, just after, or close to the respiratory peak (Lim et al. 2016).

86 Therefore, the use of ethylene biosynthesis inhibitors, such as 1-
87 Methylcyclopropene (1-MCP), would delay ripening. This approach is mainly applied to
88 climacteric fruit in order to block the ethylene receptors. 1-MCP have been used in peach
89 for alleviating chilling injury symptoms (e.g., internal browning and flesh mealiness), as
90 well as for maintaining a high level of quality in different fruit species (Jin et al. 2011).
91 Following 1-MCP treatment, reduced ethylene production, reduced respiration rate, and
92 delayed fruit softening have been commonly observed effects in kiwifruit (*Actinidia*
93 *deliciosa*), apricot (*Prunus armeniaca* L.), “aprium” fruit (*Prunus armeniaca* × *salicina*
94 L. cv. Xingmei), and ‘Bartlett’ pears (*Pyrus communis* L) (Ilina et al. 2010; Muñoz et al.
95 2012; Ma et al. 2014; Wang and Sugar et al. 2015).

96 In other cases, however, it may be desirable to accelerate the ripening of immature
97 fruit, depending on market requirements. Ethephon, known as acid-2-chloroethyl-
98 phosphonic (Ethrel®), is known for accelerating ripening in climacteric fruit, thus
99 promoting the development of fruit color and flesh softening. However, as Zhang et al.
100 (2012) have discussed, despite the usefulness of ethephon, its effects on the
101 physicochemical properties and on kiwifruit quality have not been fully unveiled.

102 Ethylene-coding genes have been intensely investigated in different fruit species,
103 including kiwifruit, *Actinidia deliciosa* (Ikoma et al. 1999, 1998; Sun et al. 2010; Xu et
104 al. 1998, 2000). In recent years, researchers have made some progress regarding the
105 possible genes related to the production of ethylene in kiwifruit using different 1-MCP
106 treatments. It has also been reported that the inhibition of the expression of KWACO1
107 and KWACS1 genes by 1-MCP is related to the inhibition of ethylene production (Ilina
108 et al. 2010). In addition, an increase of AC-ACO1, AC-ACO2, AC-SAM1, and AC-

109 SAM2 transcripts before the induction of AC-ACS1, as well as an increase in ethylene
110 production after propylene treatments, have also been reported (Mworia et al. 2010).

111 Even though today there are many available sequencing technologies, there are
112 few studies that have focused on the genes related to kiwifruit ripening based on RNA-
113 seq. RNA-seq technology utilizes pyro-sequencing, and it has been shown to sequence
114 cDNA efficiently (Shendure and Ji, 2008; Wang et al. 2009). Therefore, transcriptomic
115 analysis is a widely used tool in studies of differential gene expression, using contrasting
116 conditions or treatments, as well as different plant tissues, in order to discern genes related
117 to the fruit ripening process or genes involved in the metabolism of ethylene. Minas et al.
118 (2018) confirmed that 1-MCP and ozone acted as repressive modulators of kiwifruit
119 ripening, and Gunaseelan et al. (2019) reported new copy variants in ETHYLENE
120 RESPONSE FACTOR/APETALA2 (ERF/AP2) related to kiwifruit ripening associated
121 to cold and ethylene response.

122 In peach (*Prunus persica* L.), Wang et al. (2017a) recently used basic local
123 alignment search tool (BLAST) analysis of sequences between tomato proteins (*Solanum*
124 *lycopersicum* L.) and the peach genome database, allowing the identification of 15 genes
125 involved in ethylene signal transduction, including an ethylene ETR receptor
126 (Prupe.1G034300) and five AP2/ERF genes (Prupe.1G037700, Prupe.2G289500,
127 Prupe.3G240000, Prupe.5G061800, and Prupe.7G194400). Furthermore, previous
128 analyses of the fruit transcriptome of peach treated with 1-MCP and using microarrays
129 (μ PEACH1.0) confirmed an ethylene receptor (ETR2) and three ethylene-sensitive
130 factors (ERF), together with other transcription factors (TFs) and dependent genes of
131 ethylene, involved in changes in ripening parameters (Ziliotto et al. 2008). Additionally,
132 studies on differential gene expression related on fruit treated with 1-MCP and Ethrel®
133 have been reported in papaya (*Carica papaya* L.) (Shen et al. 2017). Ultimately, 20 genes

134 related to the cell wall and 18 related genes with chlorophyll and carotenoids were
135 identified—related to chlorophyll degradation and carotenoid metabolism inhibition—
136 were shown to play an important role in papaya coloration. In the case of persimmon,
137 fruit treated with ethylene showed a faster expression of the DKEIL, DKERF2, DKERF5,
138 and DKERF8 genes at 25 °C than at 15 °C (Park et al. 2017). In cherry tomato (*Solanum*
139 *lycopersicum* L.), 1-MCP significantly affected the biosynthesis of aromatic compounds,
140 as well as postharvest storage at low temperatures (Zou et al. 2018). In the specific case
141 of *Actinidia*, few studies have been focused on RNA-seq analysis as the work of Li et al.
142 (2015), where the gene expression profile of anthocyanin was thoroughly investigated in
143 ‘Hong Yang’ kiwifruit. Moreover, using ‘Hong Yang’ kiwifruit, Tang et al. (2016)
144 identified thousands of differentially expressed genes (DEGs) that were associated with
145 sugar metabolism, organic acid, and main amino acids.

146 The aim of the present study was to evaluate the physiological response of
147 kiwifruit, as well as the molecular mechanisms involved, under diverse conditions in
148 ripening and ethylene biosynthesis. To achieve this goal, we generated a transcriptomic
149 reference framework in the response of *Actinidia deliciosa* kiwifruit vis-à-vis harvest time
150 and the presence of 1-MCP ethylene antagonist and Ethrel®.

151 **Materials and methods**

152 *Plant material and assays*

153 In this work, ‘Hayward’ kiwifruits (*Actinidia deliciosa*) were collected from
154 six kiwifruit vines previously marked in an orchard nurseries Biotecnia© located in
155 Teno, Chile.

156 Two ripeness stages (5.2 % and 8.0 % soluble sugar content) were defined,
157 and 850 fruit were used for each ripeness stage (Tables S1 and S2). In the first
158 treatment (1-MCP), fruits were placed into two 70 L watertight polypropylene

159 chambers, and 1-Methylcyclopropene (1-MCP) was gasified as a Smart Fresh™
160 product 0.14 % (625 ppb = 0.625 µl L⁻¹) during 16 h, which was homogenized by
161 constant airflow. In the second treatment (Ethrel®), fruits were treated by dipping
162 them into a water solution with ethephon (acid-2-chloroethyl-phosphonic), applied
163 as Ethrel® 48 SL (300 µl L⁻¹). A total of twenty fruits per treatment (1-MCP and
164 Ethrel®) and day including a control (not treated fruit) were stored at 20 °C for 29
165 d. For each treatment and control, 12 kiwifruits were characterized at the beginning
166 of the trial period (at harvest= day 0; 48 hours after harvest= day 1) in the middle of
167 the study period (after 15 d), and at the end of the trial period (after 29 d or at eating
168 ripeness, when flesh reached 13 N). Fruit weight (g), diameter (three axes), the skin
169 and flesh chlorophyll index (I_{AD}), the skin and flesh color (L*a*b*), dry matter content
170 (%) and soluble solids (%) were measured. Additionally, the firmness evolution of
171 kiwifruits was monitored every 2 days during this period, including fruit firmness by
172 penetration (7.9 mm diameter plunger) of the whole fruit after removing the skin from
173 both ‘cheeks’; flesh firmness by puncture (2 mm diameter plunger) of the half fruit; and
174 core firmness by puncture (2 mm diameter plunger) which corresponds to the placental
175 tissue. Respiration rate (ml CO₂ kg⁻¹ h⁻¹) as well as kiwifruit firmness evolution was
176 monitored every two days. Finally, levels of vitamin C—as ascorbic acid (mg mL⁻¹)—
177 and organic sugar content, including glucose, fructose, and sucrose (mg mL⁻¹), were also
178 quantified.

179 I_{AD} was measured by a DA-meter (Gottardi et al. 2009); the skin and flesh colors
180 were measured with a Minolta colorimeter (CIE L*a*b*); the firmness was quantified in
181 Newton (N) by a texture analyzer (TA.XT plus); and soluble solid content (SSC) was
182 determined by a handheld ATAGO® refractometer, calibrated as the percentage of sucrose
183 at 20 °C. The respiration rate was determined by using HP 5890 SERIES II Gas

184 Chromatography System (Hewlett-Packard, 1989) using five biological replicates (five
185 fruits). As for levels of vitamin C—as ascorbic acid (mg mL^{-1})—and organic sugar
186 content, including glucose, fructose, and sucrose (mg mL^{-1}), samples were prepared from
187 three fruit halves per day, treatment, and ripeness stage, and then conserved at $-80\text{ }^{\circ}\text{C}$.
188 Juice samples were mechanically extracted with sterile gauze and stored in 2 mL tubes.
189 Subsequently, the samples were filtered using a physical filter (SLGVX13NL Millex-GV,
190 Durapore PVDF hidrof. of $0.22\text{ }\mu\text{m}$) and a chemical filter (OASIS HLB of 6 cm^3 and 30
191 μm), and stored again at $-80\text{ }^{\circ}\text{C}$ for the ascorbic acid and sugars measurements. A Hitachi
192 HPLC using Kromasil® C18 was used for the sugar determinations, and NH_2 columns
193 were used for the ascorbic acid determinations. For the sugar measurements, 5 mL of the
194 sample was prepared with 1 mL of juice, 0.5 mL of glycerol standard, and 3.5 mL of
195 doubly distilled and deionized water using 80 % acetonitrile as the mobile phase under
196 isocratic conditions according to Vicente et al. (1991).

197 These samples were transferred to amber vials to inject a volume of 20 μL using
198 an injection time of 15 min and a mobile phase flow of 1 mL min^{-1} . For the ascorbic acid
199 measurements, pure juice samples were directly transferred into amber vials for injection
200 into the HPLC. The mobile phase was used in the phosphate buffer and acetonitrile 60:40
201 (v/v) according to El Gindy et al. (2006), and the volume injected per sample was 10 μL
202 using an injection time of 6 min and a mobile phase flow of 0.8 mL min^{-1} . For the organic
203 sugar and ascorbic acid determination three samples were injected per treatment and day.

204 Finally, five fruit samples for each treatment and evaluation day were frozen for
205 RNA-seq analysis.

206 *Phenotypic data analysis*

207 Analysis of variance (ANOVA) per treatment and per day for each ripeness stage
208 was performed by comparing the mean difference by Tukey test ($\alpha < 0.05$). Pearson

1
2
3
4
5
6
7
8
9
10
11
12
13
14
15
16
17
18
19
20
21
22
23
24
25
26
27
28
29
30
31
32
33
34
35
36
37
38
39
40
41
42
43
44
45
46
47
48
49
50
51
52
53
54
55
56
57
58
59
60
61
62
63
64
65

209 correlation coefficients were also analyzed, and the effect of the treatments and time over
210 the evaluated traits was calculated by principal component analysis (PCA). In addition, a
211 general linear mixed model (GLMM) analysis was performed using the restricted
212 maximum likelihood method (REML), taking the time as the fixed variable (evaluation
213 day) and the treatments (not treated, 1-MCP and Ethrel®) as the random variables. This
214 procedure allowed us to gauge the effects of the treatments in an independent way over
215 time using best linear unbiased predictors (BLUPs). All statistical analyses were
216 calculated and edited using INFOSTAT v16 software, with the exception of the GLMM
217 analysis, which was calculated by an interface between INFOSTAT and R.

218 *Library construction and sequencing*

219 Total RNA was extracted from the fruits for each treatment (not treated, 1-MCP
220 and Ethrel®) and day (D4 and D13) using a Sigma Spectrum™ Plant Total RNA Kit.
221 Tissues for RNA extraction included flesh, core, and seeds, and three independent
222 biological replicates were used for each treatment and day, which supposed 18 RNA
223 samples for the libraries' construction. In order to quantify the RNA, a Qubit® RNA BR
224 Assay Kit was used, and to verify the RNA quality, a Fragment Analyzer Automated CE
225 System (AATI) was used. A TruSeq RNA HT Sample Prep Kit was used for library
226 construction using one microgram of the RNA sample. The libraries were sequenced
227 using a HiSeq 2500 platform according to HiSeq 2500 System User 'Guide Part 15011190
228 Rev. V HCS 2.2.70'. Raw images were generated by an Illumina HiSeq using HiSeq
229 Control Software v2.2 for system control and base calling through an integrated primary
230 analysis software called RTA (Real Time Analysis. v1.18). The base binary calls were
231 converted into FASTQ by utilizing Illumina package bcl2fastq (v1.8.4). The quality reads
232 sequencing obtained by the Illumina HiSeq 2500 were analyzed (pre-trimming) with the
233 software FastQC1 for determining the quality of sequencing. FLEXBAR2 software was

1
2
3
4
5
6
7
8
9
10
11
12
13
14
15
16
17
18
19
20
21
22
23
24
25
26
27
28
29
30
31
32
33
34
35
36
37
38
39
40
41
42
43
44
45
46
47
48
49
50
51
52
53
54
55
56
57
58
59
60
61
62
63
64
65

234 used for trimming, as well as to filter the low-quality reads (i.e., a Phred value of less than
235 25), removing the adapters, sequences with many Ns, and reads smaller than 100 bp from
236 the sequencing libraries.

237 *Alignment and gene expression analysis*

238 The sequence alignment was performed with Bowtie v2 software (Langmead et
239 al. 2012), using ‘Hong Yang’ (*Actinidia chinensis*) as the reference genome (National
240 Center for Biotechnology Information, NCBI). Samtools4 v0.1.19 was used to convert
241 the files in sequence alignment/map (SAM) format into binary alignment map (BAM)
242 format. SAM format is a generic format used to store alignments of nucleotide sequences,
243 while BAM is the compressed version of the SAM format. Transcript abundance and the
244 transcriptome assembly of each sample were created using Cufflinks5 v.2.1.13, using the
245 BAM files resulting from the alignment. The transcriptomes assembled, the annotated
246 genome, and the genome sequence of *Actinidia chinensis* (NCBI) were merged into a
247 single gtf format using the Cuffmerge tool. The Cuffdiff by differential gene expression
248 analysis and the results obtained were loaded with the CummeRbund6 visualization
249 package in order to manage, visualize, and integrate all the data produced by the Cuffdiff
250 analysis, using the statistical information environment R7 (version 3.3.3). The
251 CummeRbund6 visualization package shows the quantity versus the dispersion of all
252 genes for the different conditions (Fig. S3), the density of genes for each condition (Fig.
253 S4), the dispersion diagrams according to \log_{10} of fragments per kilobase million (FPKM)
254 (Fig. S5), and boxplots for FPKM distributions, including three biological replicates (Fig.
255 S6). Finally, we defined the cutoff point between \log_{10} (p-value) and \log_2 (fold change) for
256 each treatment (not treated fruit, T0; 1-MCP, T1; and Ethrel®, T2) and day (D4 and D13)
257 at p-value < 0.005, obtaining 18,036 DEGs from a total of 79,614 genes (Fig. S7). FPKM

1
2
3
4
5
6
7
8
9
10
11
12
13
14
15
16
17
18
19
20
21
22
23
24
25
26
27
28
29
30
31
32
33
34
35
36
37
38
39
40
41
42
43
44
45
46
47
48
49
50
51
52
53
54
55
56
57
58
59
60
61
62
63
64
65

258 were used to measure the number of transcripts of each gene, and only doubly expressed
259 genes were considered as DEGs for each treatment comparison.

260 *Gene Ontology and network analysis*

261 Gene-act-network analysis was performed to identify the interactive network
262 among the Gene Ontology (GO) terms enriched in DEGs based on the GO database using
263 the Biological Networks Gene Ontology (BiNGO) tool in Cytoscape version 3.7.2 (Maere
264 et al. 2005; Shannon et al. 2003), which calculates overrepresented GO terms in the
265 network and displays them as a network of significant GO terms. For analysis of the
266 enrichment of the metabolic pathways, the public Kyoto Encyclopedia of Genes and
267 Genomes (KEGG) database (Bindea et al. 2009, 2013) and the pathways were analyzed
268 in Cytoscape (Shannon et al. 2003) using the ClueGO (Kanehisa et al. 2016, 2017) plug-
269 in. Besides, PPI of the DEGs—associated with cellular and metabolic processes, and the
270 translation of hormonal signals,— was analyzed using the search tool for the retrieval of
271 interacting genes (STRING) (Szklarczyk et al. 2017), where a score > 0.400 was
272 considered for the DEGs. Cytoscape was used to visualize the PPI for the DEGs and to
273 identify the key genes (Shannon et al. 2003).

274 *Verification of qRT-PCR*

275 The oligonucleotide primers were designed from sequences of genes previously
276 aligned to the *Actinidia* reference genome (Huang et al. 2013) using the software Primer3
277 version 0.4.0 (Untergasser et al. 2007) (Table S12). The AGB1 (Achn005971) and
278 ACTIN 7 (Achn107351) genes were used as references. Internal data from the RNA-seq
279 was used for reference gene selection following the criteria established by Zhou et al.
280 (2017). RT-qPCR was carried out using a KAPA SYBR® FAST Universal qPCR Kit
281 (Kapa Biosystems) on an Eco Real-Time PCR System (Illumina). Each reaction mixture
282 contained 1.0 µL of cDNA, KAPA SYBR® FAST Universal qPCR Kit 5 µL, KAPA

1
2
3
4
5
6
7
8
9
10
11
12
13
14
15
16
17
18
19
20
21
22
23
24
25
26
27
28
29
30
31
32
33
34
35
36
37
38
39
40
41
42
43
44
45
46
47
48
49
50
51
52
53
54
55
56
57
58
59
60
61
62
63
64
65

283 SYBR® ROX Low (50X) 0.2 µL, PCR direct primer (10 µmol L⁻¹) 0.2 µL PCR, reverse
284 primer (10 µmol L⁻¹) 0.2 µL, and 3.4 µL ddH₂O, for a final volume of 10 µL. The PCR
285 conditions were 95 °C for 3 min, followed by 40 cycles of 95 °C for 3 s, 60 °C for 30 s,
286 and 72 °C for 35 s. The quantification of the expression level of the genes was carried out
287 using a relative quantification method, Pfaffl (Satyanarayana et al. 1984), and each
288 sample was amplified in duplicate.

289 **Results**

290 *Fruit phenotyping*

291 ‘Hayward’ kiwifruit were harvested in two ripeness stages (i.e., E1, ≈ 5 % of SSC;
292 and E2, ≈ 8 % of SSC) after four postharvest periods— at harvest (day 0), 48 h after
293 harvest (day 1), 15 d after harvest (day 15), and 29 d after harvest (day 29) (Fig. 1 and
294 Tables S1-S2)—and treated with 1-MCP and Ethrel® in order to test the effect of
295 different ethylene biosynthesis conditions in terms of fruit physiology. In general, the
296 fruit of the first harvest (E1) were more responsive to the treatments in most of the
297 evaluated traits (i.e., the skin I_{AD}, flesh I_{AD}, SSC, and flesh color) than the E2 fruit,
298 showing greater differences over time among the treatments (Fig. 1). Thus, the skin and
299 flesh I_{AD} of 1-MCP treatment showed a lower decrease due to the 1-MCP effect,
300 indicating lower chlorophyll degradation, in contrast to Ethrel®, which produced greater
301 chlorophyll degradation, and therefore, faster fruit senescence. Similar results were
302 observed for flesh color, particularly in terms of luminosity (L*; CIE L*a*b*),
303 demonstrating that the fruit from 1-MCP treatment had a lower luminosity decrease for
304 both ripeness stages with respect to not treated and Ethrel® treated fruit due to the 1-
305 MCP effect (Fig. 1). Nonetheless, it is noteworthy that in all cases, not treated and
306 Ethrel® treated fruit exceeded 1-MCP treatment in terms of SSC, which could suggest
307 that the 1-MCP effect might decrease or delay fruit sugar accumulation.

1
2
3
4
5
6
7
8
9
10
11
12
13
14
15
16
17
18
19
20
21
22
23
24
25
26
27
28
29
30
31
32
33
34
35
36
37
38
39
40
41
42
43
44
45
46
47
48
49
50
51
52
53
54
55
56
57
58
59
60
61
62
63
64
65

308 Regarding respiration rate, not treated and Ethrel® fruit produced a respiratory
309 increase in CO₂ production, unlike the 1-MCP, especially in E1 (Fig. 2). However, E2
310 showed no differences among the treatments in terms of respiratory rate, which was
311 probably due to the advanced ripeness stage. According to maximum treatment
312 differences, we highlighted Ethrel® and not treated fruit, which reached their highest
313 respiratory rate at day 4 and day 6, respectively, with values over 30 ml CO₂ kg⁻¹ h⁻¹;
314 meanwhile, 1-MCP as expected for an ethylene inhibitor remained at a low and constant
315 respiratory rate for both ripeness stages (Fig. 2). As for firmness evolution, fruit, flesh,
316 and core firmness showed significant differences between 1-MCP and Ethrel®
317 treatments, especially in E1 (Fig. 3). Regarding fruit firmness in E1, all treatments started
318 with similar values of around 80 N. It is interesting to note that 1-MCP maintained a
319 constant firmness level for several days, ranging between 70 N and 80 N, but then a
320 change in this trend starting on day 15 was noted, and ultimately reaching a firmness of
321 50 N on day 29. On the other hand, the firmness in not treated and Ethrel® fruit decreased
322 considerably throughout the whole period. The greatest loss of firmness was experienced
323 by the Ethrel® treated fruit, which reached their consumption maturity (10-15 N) on
324 around day 25, while the not treated fruit reached their consumption maturity on day 29.
325 It should be noted that the postharvest life of the fruit was much higher for the 1-MCP
326 treatment, which did not reach consumption maturity after 29 d. In addition, the greatest
327 differences in firmness between the treatments were observed on day 13, when there was
328 a difference of up to 50 N between 1-MCP and Ethrel® treatments (Fig. 3). Regarding
329 E2, the differences between the treatments were lower than E1, with almost no significant
330 differences except for day 20, where Ethrel® showed a difference of around 20 N
331 compared to not treated and 1-MCP fruit (Fig. 3).

1
2
3
4
5
6
7
8
9
10
11
12
13
14
15
16
17
18
19
20
21
22
23
24
25
26
27
28
29
30
31
32
33
34
35
36
37
38
39
40
41
42
43
44
45
46
47
48
49
50
51
52
53
54
55
56
57
58
59
60
61
62
63
64
65

332 In terms of for sugar content, we observed that 1-MCP produced a lower increase
333 in contrast to the not treated or Ethrel® fruit, as these differences were lower in the E2
334 ripeness stage (Fig. S1). In both cases, the highest concentrations ranged from 7 to 8 mg
335 mL⁻¹ of glucose and fructose. Additionally, we observed no differences between the
336 fructose and glucose levels, which showed similar concentrations (Fig. S1). As for
337 vitamin C, determined as ascorbic acid (mg mL⁻¹), there was neither a clear trend among
338 the treatments nor over time, always ranging from 0.5 to 0.7 mg mL⁻¹ (Fig. S1).

339 According to Pearson correlations, the highest value was obtained between fruit
340 firmness and SSC for both ripeness stages (-0.93 and -0.84) as well as there was another
341 important correlation in the E1 between flesh color (L*) and fruit firmness (0.89) (Tables
342 S3 and S4). Principal component analysis (PCA) of the fruit trait data showed that most
343 of the variability was explained by the first component (PC1) in terms of both treatments
344 and time, reaching 74.6 % and 92 %, respectively (Fig. 4); a significant effect of the
345 treatment over traits was noted, especially in E1, where Ethrel® treatment was related
346 to a major SSC increase, including in fructose and glucose levels, while 1-MCP had a
347 greater effect on fruit firmness, implying a lesser degree of softening and chlorophyll
348 degradation (Fig. 4).

349 In summary, after analyzing the data for all evaluated traits and ripeness stages,
350 treatments showed a greater effect in the E1 stage. This observation was supported by
351 GLMM analysis, since obtained BLUPs' coefficients indicated an inverse effect of 1-
352 MCP compared to not treated and Ethrel® fruit (Table S5). This situation resulted in a
353 less fruit softening for 1-MCP treatment and a major SSC and sugars content for not
354 treated and Ethrel® fruit. Thus, we found that the most suitable ripeness stage to evaluate
355 the differential gene expression due to treatments was E1, because of the critical
356 differences observed. Therefore, for the RNA-seq analysis, we decided to choose fruit

1
2
3
4
5
6
7
8
9
10
11
12
13
14
15
16
17
18
19
20
21
22
23
24
25
26
27
28
29
30
31
32
33
34
35
36
37
38
39
40
41
42
43
44
45
46
47
48
49
50
51
52
53
54
55
56
57
58
59
60
61
62
63
64
65

357 from E1 because there were greater differences between treatments and days compared
358 to E2. Taking into account that fruit firmness and respiration rate were the traits most
359 significantly affected by the treatments in E1 (Fig. 4 and Tables S3-S4), we selected day
360 4, according to the maximum respiration rate (Fig. 2), as well as day 13, for its maximum
361 firmness difference between the treatments (Fig. 3), since we considered.

362 *Sequencing and alignment results*

363 Supposing an average value of 37,233,093 reads per sample, we sequenced a total
364 of 670,195,682 raw reads. We learned that, on average, more than 95 % of the reads
365 showed a Phred quality score over 20 (Q20 %), and more than 90 % of the reads had a
366 quality score of over Q30 (Table S6). Thus, a total of 315,537,899 filtered reads were
367 aligned to the *Actinidia chinensis* genome (Huang et al. 2013), obtaining a 70.7 %
368 alignment, while 29.3 % were not aligned (Tables 1 and S7). In addition, 50.7 % of the
369 aligned sequences (35.87 %) were located in a unique position, while the remaining
370 sequences (34.84 %) were aligned to multiple positions. All raw reads in FASTQ format,
371 including paired-end and replicates, are available from the NCBI Short Read Archive
372 (SRA) database under BioProject number PRJNA638129.

373 *Differentially expressed genes (DEGs) and functional annotation*

374 As we previously observed, the 1-MCP and Ethrel® treatments produced an
375 expected effect that, respectively, extended and reduced the fruit's shelf-life potential. A
376 total of 18,036 genes (Fig. 5a and Table S8) were differentially expressed at p-value <
377 0.005. Moreover, in the PCA (Fig. S2), we noted more differences between the treatments
378 on day 4. In order to obtain the most significant genes, we only considered as DEGs those
379 doubly expressed in any treatment comparisons, obtaining 8,626 upregulated genes of 1-
380 MCP treatment (T1) over Ethrel® treatment (T2) in day 4, while in day 13, the number
381 of up- or downregulated genes was similar for both treatment comparisons (Fig. 5b). In

1
2
3
4
5
6
7
8
9
10
11
12
13
14
15
16
17
18
19
20
21
22
23
24
25
26
27
28
29
30
31
32
33
34
35
36
37
38
39
40
41
42
43
44
45
46
47
48
49
50
51
52
53
54
55
56
57
58
59
60
61
62
63
64
65

382 addition, we found that the number of genes per range expression was reduced
383 considerably on day 13 (Fig. S8).

384 The functional annotation of the DEGs was performed using the Gene Ontology
385 resource, whereby the genes were classified according to three criteria: biological
386 process, cellular component, and molecular function. The number of DEGs on day 4 was
387 quantitatively higher than those on day 13; however, they showed a proportional
388 similarity (Fig. 6 and Table S9). The difference was marked by treatment comparisons,
389 generating a 1-MCP (T1) versus Ethrel® (T2) enrichment on day 4, and a not treated fruit
390 (T0) versus 1-MCP (T1) on day 13. In addition, the graphic absence of a 1-MCP (T1)
391 versus Ethrel® (T2) on day 13 was due to the low number of DEGs. The terms of cellular
392 and metabolic processes were observed more frequently in the ontology of biological
393 processes; meanwhile, the terms' cell, intracellular, cytoplasm, and membrane were most
394 frequently observed in the ontology of the cellular components and in the molecular
395 functions, catalytic activity and binding activity (Fig. 6).

396 *Enrichment analysis of pathways*

397 Additionally, KEGG assignments were used to classify the functional annotations
398 for a better understanding of the biological functions and to enrich the biological path of
399 each DEG-derived transcript. At least 473 genes (Table S10) were related to different
400 metabolic pathways, *e.g.*, photosynthesis, porphyrin, and chlorophyll metabolism; plant
401 hormone signal transduction; starch and sucrose metabolism; amino sugar nucleotide
402 sugar metabolism; RNA transport; and spliceosome (Figs. 7 and S9-S16). The results
403 showed that the DEGs that participated in the route of photosynthesis and starch and
404 sucrose metabolism decreased in day 13, probably because the fruit experienced a
405 transitional period of starch accumulation characterized by the activity of key enzymes in
406 the metabolic route of sucrose, which decreased in parallel to the decrease in starch levels.

1
2
3
4
5
6
7
8
9
10
11
12
13
14
15
16
17
18
19
20
21
22
23
24
25
26
27
28
29
30
31
32
33
34
35
36
37
38
39
40
41
42
43
44
45
46
47
48
49
50
51
52
53
54
55
56
57
58
59
60
61
62
63
64
65

407 Plant hormone signal transduction, amino sugar nucleotide sugar metabolism, RNA
408 transport, and spliceosome were significantly enriched on day 4 after treatment (Fig. 7
409 and Table S10).

410 *Protein-protein interaction network of DEGs and related pathways*

411 The putative function and DEGS levels were integrated into a network of PPIs
412 using the STRING biological database, with an interaction score of > 0.7 . G6PD1, PGL1
413 and PRSI from pentose phosphate pathway were identified (Fig. 8) being PGL1 (K01057)
414 and PRSI (K00948) overexpressed in Ethrel® and 1-MCP respectively and interacting
415 with the key genes of tricarboxylic acid cycle [TCA] cycle such as E1 ALPHA, mtLPD1,
416 ACO3 and ACLB-2 being ACO3 (K01681) especially overexpressed in 1-MCP (Fig. 9
417 and Fig. S10). In turn, TCA related genes interact with GAPC2, GAPC1, and LOS2 (Fig.
418 8), which participate in glycolysis being LOS2 (K01689) overexpressed by 1-MCP at the
419 previous synthesis stage of 2-phosphoenolpyruvate (PEP) (Fig. S11). In addition, LOS2
420 interacts with genes belonging to starch and sucrose metabolism such as HKL1 and
421 APL3, and within this group, PHS2, TRE, and HXK1 were also identified (Fig. 8). In this
422 instance, APL3 (K00975) and PHS2 (K00688) were especially overexpressed in 1-MCP
423 (Fig. S12). As for pentose and glucuronate interconversions ATPME3, PMR6, UGD2 and
424 Achn209711 were identified (Fig. 8). In addition, Achn209711 (K01805) which is
425 overexpressed in 1-MCP, is in a key position interacting with glycolysis and starch and
426 sucrose metabolism (HXK1 and HKL1) while the provider of nucleotide sugars for the
427 cell wall UGD2 (K00012) is downregulated in 1-MCP and upregulated in Ethrel® (Fig.
428 S13). Moreover, PMR6 (K01728, K22539) and Achn330311 (K01051) were
429 overexpressed in Ethrel® in the pentose and glucuronate interconversions, which in turn
430 are related to the disassemble of the fruit cell wall mediated by polygalacturonase (Fig.

1
2
3
4
5
6
7
8
9
10
11
12
13
14
15
16
17
18
19
20
21
22
23
24
25
26
27
28
29
30
31
32
33
34
35
36
37
38
39
40
41
42
43
44
45
46
47
48
49
50
51
52
53
54
55
56
57
58
59
60
61
62
63
64
65

431 S13). Therefore, if we consider the most differentially expressed genes by metabolic
432 pathway, the polygalacturonase enzyme is overexpressed in Ethrel® (Fig. 9).

433 Additionally, in a separate cluster, genes involved in porphyrin and chlorophyll
434 metabolism were identified (Fig. 8), such as GUN5, ALB1, NYC1, CLH2, PORA, and
435 PORB. Genes related to multifunctional protein GUN5 (K03403), PORA (K00218), and
436 PORB (K00218) were overexpressed in 1-MCP as well as CLH2 (K08099) and NYC1
437 (K13606) which were involved in the previous steps of chlorophyll a and b synthesis (Fig.
438 S14). Therefore, we can hypothesize that 1-MCP slowed the chlorophylls degradation.
439 Moreover, GUN5 is interacting with OST1 (K14498) which links porphyrin and
440 chlorophyll metabolism with plant hormone signal transduction. EIN2 and ETR2
441 participate in plant hormonal signal transduction (Fig. 8) specifically in the cysteine and
442 methionine metabolism. In this case, ETR2 (K14509), as expected were downregulated
443 by 1-MCP and upregulated by Ethrel® in day 4 which confirms the 1-MCP and Ethrel®
444 effect over ethylene emission through both proteins (Fig. 9 and Fig. S15). As for
445 carotenoid biosynthesis, CHY2 and B2 (K15746) were interconnected in a separate
446 cluster being B2 downregulated by 1-MCP for the day 4 as it's shown in Fig. 9 and Fig.
447 S16.

448 Finally, if we analyze the genes that showed higher expression per metabolic
449 pathway in the 1-MCP vs Ethrel® comparison (Fig. 9 and Table S11), we could
450 appreciate genes encoding proteins linked to photosynthesis in photosystems a and b,
451 resulting in an overexpression by 1-MCP for PSBY (K02723) and PSBP (K02717), which
452 could show evidences of the chlorophyll–photosynthesis interrelation in fruit senescence.

453 *Confirming genes' expression using RT-qPCR*

454 In addition to the physical and chemical changes described above, a set of genes
455 involved in ripening was investigated. Fruit ripening implies physiological changes, such

1
2
3
4
5
6
7
8
9
10
11
12
13
14
15
16
17
18
19
20
21
22
23
24
25
26
27
28
29
30
31
32
33
34
35
36
37
38
39
40
41
42
43
44
45
46
47
48
49
50
51
52
53
54
55
56
57
58
59
60
61
62
63
64
65

456 as flesh softening, color change, and taste development, among other process. In
457 particular, fruits treated with 1-MCP showed differences in the expression of several
458 genes related to ripening (Fig. 10), suggesting that this endogenous ethylene inhibitor acts
459 largely independently in kiwifruit. After the application of 1-MCP, the expression of
460 certain negative ethylene regulators genes involved in the starch and sucrose metabolism
461 (ATSPS4F, Achn218701), porphyrin and chlorophyll (CHLM, Achn271251) and citrate
462 cycle (ACO3, Achn152281) increased.

463 In addition, as we have shown the application of 1-MCP can delay the degradation
464 of chlorophyll being fruit color largely determined by the presence of chlorophyll and
465 carotenoids (McGhie et al. 2002). This delay in chlorophyll degradation is associated with
466 inhibition of ethylene production by suppressing the gene expression of PAO, NYC
467 (Achn069361), NOL, and SGR1, which are closely associated with the chlorophyll
468 catabolic pathway (Cheng et al. 2012), thus increasing the expression of CHLM
469 (Achn271251) and CRD1 (Achn328501).

470 Ethrel® treatment was found to stimulate polygalacturonase (Achn051381)
471 synthesis, while 1-MCP treatment delayed fruit maturation and polygalacturonase
472 synthesis. Besides, PRF3 (Achn163471) linked to regulation of actin cytoskeleton was
473 overexpressed in day 4 of 1-MCP treatment since it would be participating in the
474 polymerization of actin filaments.

475 **Discussion**

476 *Fruit phenotyping*

477 According to the phenotyping results discussed above, most of the evaluated traits,
478 including skin I_{AD}, flesh I_{AD}, SSC, and flesh color, showed higher differences. This was
479 particularly the case for E1, the first ripeness stage, probably due to the more advanced

1
2
3
4
5
6
7
8
9
10
11
12
13
14
15
16
17
18
19
20
21
22
23
24
25
26
27
28
29
30
31
32
33
34
35
36
37
38
39
40
41
42
43
44
45
46
47
48
49
50
51
52
53
54
55
56
57
58
59
60
61
62
63
64
65

480 physiological ripeness stage in E2. Moreover, not treated and Ethrel® treated fruit
481 favored a major SSC, including the main sugars in *Actinidia deliciosa*, fructose and
482 glucose (Nishiyama et al. 2008), as well, since greater fruit softening and chlorophyll
483 degradation is contrary to 1-MCP treatment. A previous study in ‘Qinmei’ kiwifruit,
484 suggested that applications of high concentrations of 1-MCP affected consumer
485 acceptance due to excessive sourness, but not because of fruit firmness or SSC (Deng et
486 al. 2015). As for ascorbic acid content, it did not show a clear trend either between
487 treatments or between days. Lim et al. (2016) claimed that the decrease in ascorbic acid
488 and phenolic compounds in kiwifruit is associated with longer cold storage times.

489 In addition, in the present study, a significant respiratory increase was shown for
490 not treated and Ethrel® treated fruit in days 4 and 6 compared to 1-MCP treatment, which
491 remained at a low and constant respiratory rate. This respiratory increase may be related
492 to the beginning of ethylene emission, which can occur either before or after it (Lim et al.
493 2016). An increase of ethylene approximately one week after harvest was reported by
494 Ilina et al. (2010) in ‘Hayward’ kiwifruit, which coincides with the respiratory increase
495 obtained for the not treated fruit observed in this trial. Thus, the results we obtained
496 allowed us by BLUP coefficients to select fruit firmness and respiratory rate as the most
497 determining traits in the fruit maturation process. For sequencing analysis, we selected
498 fruit from day 4 in E1, which coincided with the maximum respiratory rate, and day 13,
499 when the maximum fruit firmness difference was shown. As for E2, no fruit were selected
500 due to the small differences between the treatments.

501 *Sequencing and alignment results*

502 In terms of sequencing and alignment results, we based our bioinformatics work
503 on one of the few currently available molecular tools, i.e., the diploid kiwifruit ‘Hong
504 Yang’ (*A. chinensis*), used as a reference genome (Huang et al. 2013; Wu et al. 2019).

1
2
3
4
5
6
7
8
9
10
11
12
13
14
15
16
17
18
19
20
21
22
23
24
25
26
27
28
29
30
31
32
33
34
35
36
37
38
39
40
41
42
43
44
45
46
47
48
49
50
51
52
53
54
55
56
57
58
59
60
61
62
63
64
65

505 Although there is a ploidy difference between this cultivar and commercially important
506 varieties, there are many transcriptomic studies that have attempted to bring a greater
507 fundamental understanding with respect to disease resistance, most especially
508 *Pseudomonas syringae* (Wang et al. 2017b, 2018; Michelotti et al. 2018; Song et al.
509 2019). However, from the fruit quality or postharvest points of view, there are few studies
510 available (Tang et al. 2016; Zhang et al. 2018; Gan et al. 2020). The sequencing results
511 of our work have shown to be of high quality according to the Phred values, even
512 obtaining a high alignment result ($\approx 70\%$) with respect to the diploid reference genome,
513 which indicates a high synteny between *Actinidia chinensis*, even between different
514 species, such as *A. eriantha* (Tang et al. 2019), despite the hexaploid character of the
515 ‘Hayward’ variety.

516 *Differentially expressed genes (DEGs) and functional annotation*

517 Gene expression analysis provided a total of 18,036 DEGs, most of which were
518 expressed by day 4. This suggests that the most important changes in the fruit maturation
519 process at the physiological and biochemical levels are taking place in the first few days
520 after harvest. In contrast, the differences between 1-MCP and Ethrel® treatments were
521 minimal for day 13, indicating a reduced effect of 1-MCP during the postharvest period.
522 In order to gain a better understanding the biological functions related to the most
523 important genes, KEGG pathways were used to relate each DEG-derived transcript being
524 several genes linked to starch and sucrose metabolism; amino sugar nucleotide sugar
525 metabolism; photosynthesis, porphyrin, and chlorophyll metabolism; plant hormone
526 signal transduction; RNA transport; or spliceosome. The most significant difference
527 between treatments we found was in the porphyrin and chlorophyll metabolism activity
528 for day 4, indicating a major fruit softening rate due to the chlorophyll breakdown in not
529 treated and Ethrel® treated fruit, which also occur in the ripening process of many fruit,

1
2
3
4
5
6
7
8
9
10
11
12
13
14
15
16
17
18
19
20
21
22
23
24
25
26
27
28
29
30
31
32
33
34
35
36
37
38
39
40
41
42
43
44
45
46
47
48
49
50
51
52
53
54
55
56
57
58
59
60
61
62
63
64
65

530 including banana (*Musa acuminata*) and tomato (*Solanum lycopersicum*) (Guyer et al.
531 2014). Contrary to other fruit crops, green-fleshed varieties of kiwifruit only lose some
532 of their chlorophyll during prolonged storage (Burdon and Lallu, 2011) or when applying
533 accelerating treatments of ethylene biosynthesis by using Ethrel®, as we did in this study.

534 *Protein-protein interaction network of DEGs and related pathways*

535 PPI network revealed significant interconnections differentiated into two main
536 clusters: (1) pentose phosphate pathway, citrate cycle, glycolysis and gluconeogenesis,
537 starch and sucrose metabolism and pentose glucuronate interconversions and (2)
538 porphyrin and chlorophyll metabolism. E1 ALPHA, mtLPD1, ACO3 and ACLB-2 from
539 citrate cycle interact with GAPC2, GAPC1, and LOS2 from glycolysis and
540 gluconeogenesis. LOS2 (K01689) was overexpressed by 1-MCP at the previous synthesis
541 stage of 2-phosphoenolpyruvate (PEP) while the pyruvate decarboxylase enzyme PDC2
542 (K01568) was found to be overexpressed for the Ethrel® treatment. Therefore, both
543 related genes are linked to the oxidative decarboxylation process of pyruvic acid to
544 acetaldehyde (pyruvate decarboxylase) and pyruvate to acetate (pyruvate dehydrogenase)
545 is catalyzed by both enzymes releasing CO₂. For this reason, we found differences in the
546 kiwifruit's CO₂ emissions between the 1-MCP and Ethrel® treatments, indicating that the
547 1-MCP treatment can interfere in the transcriptional control of respiration by maintaining
548 lower rates in kiwifruit.

549 As for starch and sucrose metabolism APL3 (K00975) and PHS2 (K00688) were
550 overexpressed in 1-MCP, even ATSPS4F (K00696) which could be correlated with
551 sucrose synthesis during ripening; this is possibly due to the accumulation of starch in the
552 flesh, which, through a disassembly mechanism, can provide a carbon source for the
553 synthesis of sugars during ripening, including sucrose (Nogueira et al. 2012).

1
2
3
4
5
6
7
8
9
10
11
12
13
14
15
16
17
18
19
20
21
22
23
24
25
26
27
28
29
30
31
32
33
34
35
36
37
38
39
40
41
42
43
44
45
46
47
48
49
50
51
52
53
54
55
56
57
58
59
60
61
62
63
64
65

554 According to pentose and glucuronate interconversions, in the PPI network
555 Achn209711 (K01805) was overexpressed by 1-MCP treatment and this gene interacts
556 with glycolysis and starch and sucrose metabolism (HXK1 and HKL1) while UGD2
557 (K00012) is overexpressed by Ethrel® treatment favoring the supply of nucleotide sugars
558 for the cell wall. The pectinesterase enzyme Achn330311 (K01051) is the first enzyme in
559 the process by which Poly (1,4- α -galacturonide) is converted into Poly (1,4- α -
560 galacturonide) (n) as a prior step to its conversion to digalacturonate through the
561 polygalacturonase (K01184 [3.2.1.15]). In our trial, the enzyme pectinesterase was
562 overexpressed by the Ethrel® treatment. This enzyme belongs to the pectinases group,
563 which, as reported by Paniagua et al. (2014), is usually involved in fruit softening,
564 whereby pectins play an important role in the cell wall disassembly. In addition, lower
565 cell wall degradation has been described in plums after 1-MCP treatment especially for
566 pectinesterase, polygalacturonase, cellulase, and β -galactosidase enzymes and a higher
567 content of cell wall polysaccharide was detected (Lin et al. 2018). In addition,
568 polygalacturonase enzymes that degrade the cell wall (EC 3.2.1.15) are involved in flesh
569 softening. A kinetics study related to ethylene evolution and polygalacturonase synthesis
570 demonstrated that the evolution of ethylene preceded the synthesis of polygalacturonase
571 at 20 h (Grierson and Tucker, 1983).

572 The green color of the kiwifruit pericarp is mainly determined by the different
573 concentrations and proportions of carotenoids and chlorophyll (McGhie and Ainge,
574 2002). The applications of ethylene affected the color of the fruit, showing changes in the
575 color of the flesh and a loss of luminosity, through the inhibition of chlorophyll
576 metabolism. Chlorophyll biosynthesis enzymes are part of this process, such as
577 protochlorophyllide reductase A (PORA), protoporphyrinogen oxidase (HEMG2),
578 magnesium-chelatase subunit ChlH (CHLH), and cardiolipin synthase (CRD1), as well

1
2
3
4
5
6
7
8
9
10
11
12
13
14
15
16
17
18
19
20
21
22
23
24
25
26
27
28
29
30
31
32
33
34
35
36
37
38
39
40
41
42
43
44
45
46
47
48
49
50
51
52
53
54
55
56
57
58
59
60
61
62
63
64
65

579 as chlorophyll degradation enzymes, such as chlorophyll degradation (CLH2) and
580 robbable chlorophyll (ide) b reductase NYC1 (NYC1). In contrast, we found that the
581 application of 1-MCP increased the transcription of these enzymes. However, in the route
582 of carotenoid biosynthesis, the gene related to BETA-HIDROXILASE 1 protein (B2) was
583 downregulated after treatment with 1-MCP, decreasing its expression in 1-MCP, and
584 increasing its expression via ethylene in Ethrel® treatment.

585 Plant hormone signal transduction and the MAPK signaling pathway are both
586 other metabolic pathways affected by treatments. In our study, the kiwifruit gene
587 Achn067861 (K14509) was overexpressed after the Ethrel® treatment, contrary to 1-
588 MCP. This gene encodes the ethylene receptor [ETR2; EC2.7.13], which is involved in
589 the metabolism of cysteine and methionine, catalyzing the onset of serine/threonine-
590 protein kinase (CTR1; [EC: 2.7.11.1]), and it is responsible for fruit senescence. Other
591 studies have reported several TFs that are also involved in fruit ripening and ethylene
592 biosynthesis, some of which include MADS-box, AP2 / ERF, NAC domain, and
593 homeobox HD-Zip family proteins (Liu et al. 2015; Ma et al. 2014; Wang et al. 2017a).

594 Finally, we could assert that fruit ripeness is a very complex process which implies
595 many pathways such as pentose and glucoronate interconversions, glycolysis or starch
596 and sucrose metabolism on the one side and porphyrin and chlorophyll metabolism in the
597 other hand. Moreover, the interrelations within them through plant hormonal signal
598 transduction are critical especially for cysteine and methionine metabolism where
599 ethylene is finally released triggering a series of biological processes that favor fruit
600 senescence. In addition, the evidence of genes that encode proteins linked to
601 photosynthesis in the present study as PSBY, PSBA or PSBP are indicating that the
602 slowdown in the degradation of chlorophylls by 1-MCP would also affect other
603 photosystem II-related proteins even though the fruit is not in a photosynthetic stage. In

1
2
3
4
5
6
7
8
9
10
11
12
13
14
15
16
17
18
19
20
21
22
23
24
25
26
27
28
29
30
31
32
33
34
35
36
37
38
39
40
41
42
43
44
45
46
47
48
49
50
51
52
53
54
55
56
57
58
59
60
61
62
63
64
65

604 previous studies, the photosystems' involvement in the fruit maturation process has not
605 yet been clarified at pre-harvest level. However, at post-harvest level a possible
606 implication of photosystems would not make sense so far. For example, in tomato,
607 Carrara et al. (2001) found that the fruit showed no CO₂ assimilation in the pre-harvest
608 period; however, these authors found that the fruit tissues exhibited consistent
609 photochemical activity. In a more recent study, Lytovchenko et al. (2011) asserted that
610 tomato fruit photosynthesis is apparently not important in the ripeness process, but that it
611 does play a significant role in seed development. Even more recently, Ceusters et al.
612 (2018) summarized evidence showing that ethylene acts as a regulator of photosynthesis
613 and its associated components, such as stomatal conductance, chlorophyll, light reactions,
614 carboxylation, carbohydrate partitioning, and age-related leaves senescence of
615 *Arabidopsis*, which could explain the chlorophyll degradation and the fruit senescence
616 from the Ethrel® treatment, as well as the opposite effect from the 1-MCP treatment.
617 Therefore, the degree of involvement of these phytohormones on photosynthesis and their
618 interrelations with fruit ripening are still unknown. Thus, the study of non-coding RNA's
619 like miRNA could be an interesting approach because in climacteric fruit as tomato some
620 miRNA targets play an important role on fruit development and ripening (Karlova et al.,
621 2013) as well as in non-climacteric fruit such as strawberry (Xu et al., 2013) which
622 identified miRNA targets associated to fruit senescence through NAC transcription
623 factors or Auxin response factors (ARF) and Myb transcription factors.

624 **Conclusions**

625 This study allowed us to identify genes related to the fruit ripening of 'Hayward'
626 kiwifruit. This work is useful for creating a gene reference framework to focus on new
627 trials of other *Actinidia* species. Fruit ripening is a complex process that requires the
628 participation of biochemical, genetic, and hormonal signals. Application of exogenous

1
2
3
4
5
6
7
8
9
10
11
12
13
14
15
16
17
18
19
20
21
22
23
24
25
26
27
28
29
30
31
32
33
34
35
36
37
38
39
40
41
42
43
44
45
46
47
48
49
50
51
52
53
54
55
56
57
58
59
60
61
62
63
64
65

629 ethylene accelerates ripening, as it triggers the metabolic processes responsible for the
630 fruit's growth and maturation. This step also involves the disassembly of the cell wall,
631 which is a result of the breaking up of the sugar chains, the pigment changes, and the
632 release of aromatic compounds. In the present study, 1-MCP proved to be effective in
633 delaying fruit ripening by inhibiting the ethylene receptors, which prevents the coupling
634 of ethylene. These changes are also expressed at the molecular level, involving many
635 related pathways which are grouped in two main clusters: (1) pentose and glucuronate,
636 citrate cycle, glycolysis and gluconeogenesis or starch and sucrose metabolism and (2)
637 porphyrin and chlorophyll metabolism. Thus, increased knowledge of enzymes or
638 proteins variations related to chlorophyll content caused by ethephon, 1-MCP or even
639 over time during kiwifruit shelf-life period, could allow for a more complete
640 understanding of fruit ripening. Therefore, it would be an interesting approach to consider
641 studies on the chlorophyll evolution and even photosynthetic activity on fruit species
642 throughout the development of the fruit in the pre-harvest period, which could be related
643 to a longer or shorter fruit shelf-life in the post-harvest period. This could be an interesting
644 line of investigation for more concretely discerning the physiological mechanisms
645 involved in the fruit maturation process.

646 Ultimately, our results allow us to visualize the key genes involved in this process.
647 However, since fruit ripening is a complex process and involves more than one metabolic
648 pathway, the miRNA analysis, and even an epigenetic approach, such as methylation,
649 could complement our findings here, creating a much more complete picture of the entire
650 fruit ripening process.

651
652

1
2
3
4
5
6
7
8
9
10
11
12
13
14
15
16
17
18
19
20
21
22
23
24
25
26
27
28
29
30
31
32
33
34
35
36
37
38
39
40
41
42
43
44
45
46
47
48
49
50
51
52
53
54
55
56
57
58
59
60
61
62
63
64
65

653 **Acknowledgments**

654 The authors would like to thank to National Commission for Scientific and Technological
655 Research (CONICYT) of Chile government through the project FONDEF N° D09i-1136.
656 Additionally, we thank the Seneca Foundation in the region of Murcia (Spain) through the
657 Regional subprogramme “Saavedra Fajardo” (20397/SF/17) and Ministry of Science and
658 Innovation through the project “Juan de la Cierva Incorporación” N° IJC2018-0366-I.

659 **Data Archiving Statement**

660 Raw reads of the present RNAseq study has been uploaded in the National Center for
661 Biotechnology (NCBI), including a total of eighteen libraries in FASTQ format. These
662 libraries include paired-end reads and three biological replicates for treatments (not
663 treated fruit, T0; 1-MCP, T1; and Ethrel®, T2) and days (D4 and D13). The database is
664 available in the NCBI Short Read Archive (SRA) under BioProject number
665 PRJNA638129.

666 **References**

- 667 Atkinson RG, Cipriani G, Whittaker DJ, Gardner RC (1997) The allopolyploid origin of kiwifruit,
668 *Actinidia deliciosa* (Actinidiaceae). *Pl Syst Evol* 205, 111–124.
669 <https://doi.org/10.1007/BF00982801>
- 670 Bindea G, Galon J, Mlecnik B (2013) CluePedia Cytoscape plugin: pathway insights using
671 integrated experimental and in silico data. *Bioinformatics* 29, 661–3.
672 <https://doi.org/10.1093/bioinformatics/btt019>
- 673 Bindea G, Mlecnik B, Hackl H, Charoentong P, Tosolini M, Kirilovsky A, Fridman WH, Pagès
674 F, Trajanoski Z, Galon J (2009) ClueGO: a Cytoscape plug-in to decipher functionally grouped
675 gene ontology and pathway annotation networks. *Bioinformatics* 25, 1091–3.
676 <https://doi.org/10.1093/bioinformatics/btp101>
- 677 Burdon J, Lallu N (2011) Kiwifruit (*Actinidia spp.*). In: Yahia EM (ed) Postharvest biology and
678 technology of tropical and subtropical fruit, vol 3. Cocona to mango. Woodhead Publishing
679 Limited, Cambridge, England, pp 326–360
- 680 Carrara S, Pardossi A, Soldatini GF, Tognoni F, Guidi L (2001) Photosynthetic Activity of
681 Ripening Tomato Fruit. *Photosynthetica* 39, 75–78. <https://doi.org/10.1023/A:1012495903093>

- 682 Ceusters J, Van de Poel B (2018) Ethylene Exerts Species-Specific and Age-Dependent Control
683 of Photosynthesis. *Plant Physiology* 176, 2601 LP – 2612. <https://doi.org/10.1104/pp.17.01706>
- 684 Cheng Y, Dong Y, Yan H, Ge W, Shen C, Guan J, Liu L, Zhang Y (2012) Effects of 1-MCP on
685 chlorophyll degradation pathway-associated genes expression and chloroplast ultrastructure
686 during the peel yellowing of Chinese pear fruits in storage. *Food Chem.* 135, 415–422.
687 <https://doi.org/10.1016/j.foodchem.2012.05.017>
- 688 Datson PM, Ferguson AR (2011) *Actinidia*, in: *Wild Crop Relatives: Genomic and Breeding*
689 *Resources*. Springer Berlin Heidelberg, pp. 1–20. https://doi.org/10.1007/978-3-642-20447-0_1
- 690 Deng L, Jiang CZ, Mu W, Wang Q (2015) Influence of 1-MCP treatments on eating quality and
691 consumer preferences of ‘Qinmei’ kiwifruit during shelf life. *Journal of Food Science and*
692 *Technology* 52, 335–342. <https://doi.org/10.1007/s13197-013-0986-y>
- 693 El Gindy A, Emara S, Mostafa A (2006) Application and validation of chemometrics-assisted
694 spectrophotometry and liquid chromatography for the simultaneous determination of
695 sixcomponent pharmaceuticals. *J Pharm Biomed Anal.* 41(2): 421–30
- 696 Gan Z, Shan N, Fei L, Wan C, Chen J (2020) Isolation of the 9-cis-epoxycarotenoid dioxygenase
697 (NCED) gene from kiwifruit and its effects on postharvest softening and ripening. *Scientia*
698 *Horticulturae* 261, 109020. <https://doi.org/https://doi.org/10.1016/j.scienta.2019.109020>
- 699 Gottardi F, Noferini M, Fiori G, Barbanera M, Mazzini C, Costa G (2009) “The index of
700 absorbance difference (IAD) as a tool for segregating peaches and nectarines into homogeneous
701 classes with different shelf-life and consumer acceptance,” in *Proceedings of the 8th Pangborn*
702 *Sensory Science Symposium*. Firenze
- 703 Grierson D, Tucker GA (1983) Timing of ethylene and polygalacturonase synthesis in relation to
704 the control of tomato fruit ripening. *Planta* 157, 174–179. <https://doi.org/10.1007/BF00393652>
- 705 Gunaseelan K, McAtee PA, Nardoza S, Pidakala P, Wang R, David K, Burdon J, Schaffer RJ
706 (2019) Copy number variants in kiwifruit ETHYLENE RESPONSE FACTOR/APETALA2
707 (ERF/AP2)-like genes show divergence in fruit ripening associated cold and ethylene responses
708 in C-REPEAT/DRE BINDING FACTOR-like genes. *PLoS One.* 14(5):e0216120. doi:
709 10.1371/journal.pone.0216120. PMID: 31083658; PMCID: PMC6513069.
- 710 Guyer L, Schelbert S, Christ B, Lira B, Rossi M, Hortensteiner S (2014) Different Mechanisms
711 Are Responsible for Chlorophyll Dephytylation during Fruit Ripening and Leaf Senescence in
712 Tomato. *Plant physiology* 166. <https://doi.org/10.1104/pp.114.239541>
- 713 Hewlett-Packard (1989) Floating measurements and guarding. Application note number 123, 2nd
714 edn, Hewlett-Packard, Palo alto, CA.
- 715 Huang S, Ding J, Deng D, Tang W, Sun H, et al. (2013) Draft genome of the kiwifruit *Actinidia*
716 *chinensis*. *Nat. Commun.* 4, 1–9. <https://doi.org/10.1038/ncomms3640>
- 717 Ikoma Y, Yano M, Chuan Xu Z, Ogawa K (1998) Reduction in ethylene synthesis in
718 parthenocarpic *Actinidia deliciosa* fruit induced by N-(2-chloro-4-pyridyl)-N'-phenylurea.
719 *Postharvest Biol. Technol.* 13, 121–129. [https://doi.org/10.1016/S0925-5214\(98\)00002-7](https://doi.org/10.1016/S0925-5214(98)00002-7)

- 1 720 Ikoma Y, Yano M, Xu ZC, Ogawa K (1999) Isolation of a cDNA encoding active protein for
2 721 kiwifruit ACC synthase and its specific expression in the outer pericarp. J. Japanese Soc. Hortic.
3 722 Sci. 68, 286–288. <https://doi.org/10.2503/jjshs.68.286>
- 4 723 Iina N, Alem HJ, Pagano EA, Sozzi GO (2010) Postharvest Biology and Technology Suppression
5 724 of ethylene perception after exposure to cooling conditions delays the progress of softening in
6 725 ‘Hayward’ kiwifruit. Postharvest Biology and Technology, 55, 160–168.
7 726 <https://doi.org/10.1016/j.postharvbio.2009.11.005>
- 8 727 Jin P, Shang H, Chen J, Zhu H, Zhao Y, Zheng Y (2011) Effect of 1-Methylcyclopropene on
9 728 Chilling Injury and Quality of Peach Fruit during Cold Storage. Journal of Food Science, 76, 0–
10 729 6. <https://doi.org/10.1111/j.1750-3841.2011.02349.x>
- 11 730 Kanehisa M, Sato Y, Kawashima M, Furumichi M, Tanabe M (2016) KEGG as a reference
12 731 resource for gene and protein annotation. Nucleic Acids Res. 44, D457–D462.
13 732 <https://doi.org/10.1093/nar/gkv1070>
- 14 733 Kanehisa, M, Furumichi M, Tanabe M, Sato Y, Morishima K (2017) KEGG: New perspectives
15 734 on genomes, pathways, diseases and drugs. Nucleic Acids Res. 45, D353–D361.
16 735 <https://doi.org/10.1093/nar/gkw1092>
- 17 736 Karlova, R., van Haarst, J.C., Maliepaard, C., van de Geest, H., Bovy, A.G., Lammers, M.,
18 737 Angenent, G.C., de Maagd, R.A., 2013. Identification of microRNA targets in tomato fruit
19 738 development using high-throughput sequencing and degradome analysis. Journal of Experimental
20 739 Botany 64, 1863–1878. <https://doi.org/10.1093/jxb/ert049>
- 21 740 Langmead B, Salzberg S (2012) Fast gapped-read alignment with Bowtie 2. Nature Methods.
22 741 2012, 9:357-359. <https://doi.org/10.1038/nmeth.1923>
- 23 742 Li W, Liu Y, Zeng S, Xiao G, Wang G, Wang Y, Peng M, Huang H (2015) Correction: Gene
24 743 Expression Profiling of Development and Anthocyanin Accumulation in Kiwifruit (*Actinidia*
25 744 *chinensis*) Based on Transcriptome Sequencing. PLoS One 10, e0138743.
26 745 <https://doi.org/10.1371/journal.pone.0138743>
- 27 746 Lim S, Hyun S, Kim J, Jun H, Gu J, Jin E (2016) Inhibition of hardy kiwifruit (*Actinidia aruguta*)
28 747 ripening by 1-methylcyclopropene during cold storage and anticancer properties of the fruit
29 748 extract. Food Chem. 190, 150–157. <https://doi.org/10.1016/j.foodchem.2015.05.085>
- 30 749 Lin Yifen, Lin Yixiong, Lin H, Lin M, Li H, Yuan F, Chen Y (2018) Effects of paper containing
31 750 1-MCP postharvest treatment on the disassembly of cell wall polysaccharides and softening in
32 751 Younai plum fruit during storage. Food Chem. 264, 1–8.
33 752 <https://doi.org/10.1016/j.foodchem.2018.05.031>
- 34 753 Liu Y, Li D, Yan L, Huang H (2015) The Microgeographical Patterns of Morphological and
35 754 Molecular Variation of a Mixed Ploidy Population in the Species Complex *Actinidia chinensis* 1–
36 755 15. PLoS ONE 10(2): e0117596. <https://doi.org/10.1371/journal.pone.0117596>
- 37 756 Lytovchenko A, Eickmeier I, Pons C, Osorio S, Szecowka M, Lehmborg K, Arrivault S, Tohge
38 757 T, Pineda B, Anton M, Hedtke B, Lu Y, Fisahn J, Bock R, Stitt M, Grimm B, Granell A, Fernie
39 758 A (2011) Tomato Fruit Photosynthesis Is Seemingly Unimportant in Primary Metabolism and
40
41
42
43
44
45
46
47
48
49
50
51
52
53
54
55
56
57
58
59
60
61
62
63
64
65

- 759 Ripening but Plays a Considerable Role in Seed Development. *Plant physiology* 157, 1650–1663.
760 <https://doi.org/10.1104/pp.111.186874>
- 761 Ma L, Cao J, Xu L, Zhang X, Wang Z, Jiang W (2014) *Scientia Horticulturae* Effects of 1-
762 methylcyclopropene in combination with chitosan oligosaccharides on post-harvest quality of
763 aprium fruits. *Sci. Hortic.* (Amsterdam). 179, 301–305.
764 <https://doi.org/10.1016/j.scienta.2014.09.052>
- 765 Maere S, Heymans K, Kuiper M (2005) BiNGO: a Cytoscape plugin to assess overrepresentation
766 of Gene Ontology categories in Biological Networks. *Bioinformatics* 21, 3448–3449.
767 <https://doi.org/10.1093/bioinformatics/bti551>
- 768 McGhie TK, Ainge GD (2002) Color in fruit of the genus *Actinidia*: Carotenoid and chlorophyll
769 compositions. *J. Agric. Food Chem.* 50, 117–121. <https://doi.org/10.1021/jf0106771>
- 770 Michelotti V, Lamontanara A, Buriani G, Orrù L, Cellini A, Donati I, Vanneste JL, Cattivelli L,
771 Tacconi G, Spinelli F (2018) Comparative transcriptome analysis of the interaction between
772 *Actinidia chinensis* var. *chinensis* and *Pseudomonas syringae* pv. *actinidiae* in absence and
773 presence of acibenzolar-S-methyl. *BMC Genomics* 19, 585. [https://doi.org/10.1186/s12864-018-](https://doi.org/10.1186/s12864-018-4967-4)
774 4967-4
- 775 Minas IS, Tanou G, Krokida A, Karagiannis E, Belghazi M, Vasilakakis M, Papadopoulou KK,
776 Molassiotis A (2018) Ozone-induced inhibition of kiwifruit ripening is amplified by 1-
777 methylcyclopropene and reversed by exogenous ethylene. *BMC Plant Biol.* 18(1):358. doi:
778 10.1186/s12870-018-1584-y. PMID: 30558543; PMCID: PMC6296049.
- 779 Muñoz-Robredo P, Rubio P, Infante R, Campos-Vargas R, Manríquez D, González-Agüero M,
780 & Defilippi BG (2012) Ethylene biosynthesis in apricot: Identification of a ripening-related 1-
781 aminocyclopropane-1-carboxylic acid synthase (ACS) gene. *Postharvest Biology and*
782 *Technology*, 63(1), 85–90. <http://doi.org/10.1016/j.postharvbio.2011.09.001>
- 783 Mworia EG, Yoshikawa T, Yokotani N, Fukuda T, Suezawa K, Ushijima K, Nakano R, Kubo Y
784 (2010) Characterization of ethylene biosynthesis and its regulation during fruit ripening in
785 kiwifruit, *Actinidia chinensis* ‘Sanuki Gold’. *Postharvest Biology and Technology*, 55(2), 108–
786 113. <https://doi.org/10.1016/j.postharvbio.2009.08.007>
- 787 Nishiyama I, Fukuda T, Shimohashi A, Oota T (2008) Sugar and Organic Acid Composition in
788 the Fruit Juice of Different *Actinidia* Varieties. *Food Science and Technology Research*, 14(1),
789 67–73. <https://doi.org/10.3136/fstr.14.67>
- 790 Nogueira SB, Labate CA, Gozzo FC, Pilau EJ, Lajolo FM, Oliveira do Nascimento JR (2012)
791 Proteomic analysis of papaya fruit ripening using 2DE-DIGE. *J. Proteomics* 75, 1428–1439.
792 <https://doi.org/10.1016/j.jprot.2011.11.015>
- 793 Paniagua C, Posé S, Morris VJ, Kirby AR, Quesada MA, Mercado JA (2014) Fruit softening and
794 pectin disassembly: an overview of nanostructural pectin modifications assessed by atomic force
795 microscopy. *Annals of botany* 114, 1375–1383. <https://doi.org/10.1093/aob/mcu149>
- 796 Park D, Tilahun S, Heo JY, Jeong C (2017) Quality and expression of ethylene response genes of
797 ‘Daebong’ persimmon fruit during ripening at different temperatures. *Postharvest Biology and*
798 *Technology* 133, 57–63. <https://doi.org/10.1016/j.postharvbio.2017.06.011>

799 Park YS, Im MH, Gorinstein S (2015) Shelf life extension and antioxidant activity of ‘Hayward’
800 kiwi fruit as a result of prestorage conditioning and 1-methylcyclopropene treatment. *J Food Sci*
801 *Technol*, 52(5):2711-20. <https://doi.org/10.1007/s13197-014-1300-3>

802 Rhodes MJC (1980) Respiration and Senescence of Plant Organs, in: *Metabolism and*
803 *Respiration*. Elsevier, pp. 419–462. <https://doi.org/10.1016/b978-0-12-675402-5.50016-7>

804 Satyanarayana P, Ossakow SL, Huba JD, Guzdar PN (1984) Rayleigh-Taylor Instability in the
805 Presence of a Stratified Shear Layer. *J. Geophys. Res.* 89, 2945–2954.
806 <https://doi.org/10.1029/JA089iA05p02945>

807 Seymour GB, Taylor JE, Tucker GA (1993) *Biochemistry of Fruit Ripening* | G.B. Seymour
808 Springer. <https://doi.org/10.1007/978-94-011-1584-1>

809 Shannon P, Markiel A, Ozier O, Baliga NS, Wang JT, Ramage D, Amin N, Schwikowski B,
810 Ideker T (2003) Cytoscape: a software environment for integrated models of biomolecular
811 interaction networks. *Genome Res.* 13, 2498–504. <https://doi.org/10.1101/gr.1239303>

812 Shen YH, Lu BG, Feng L, Yang FY, Geng JJ, Ming R, Chen XJ (2017) Isolation of ripening-
813 related genes from ethylene/1-MCP treated papaya through RNA-seq. *BMC Genomics* 18, 1–13.
814 <https://doi.org/10.1186/s12864-017-4072-0>

815 Shendure J, Ji H (2008) Next-generation DNA sequencing. *Nat. Biotechnol.*
816 <https://doi.org/10.1038/nbt1486>

817 Song Y, Sun L, Lin M, Chen J, Qi X, Hu C, Fang J (2019) Comparative transcriptome analysis
818 of resistant and susceptible kiwifruits in response to *Pseudomonas syringae* pv. *Actinidiae* during
819 early infection. *PLOS ONE* 14, e0211913

820 Sun JJ, Li F, Li X, Liu XC, Rao GY, Luo JC, Wang DH, Xu ZH, Bai SN (2010) Why is ethylene
821 involved in selective promotion of female flower development in *cucumber*? *Plant Signal. Behav.*
822 5, 1052–1056. <https://doi.org/10.4161/psb.5.8.12411>

823 Szklarczyk D, Morris JH, Cook H, Kuhn M, Wyder S, Simonovic M, Santos A, Doncheva NT,
824 Roth A, Bork P, Jensen LJ, Von Mering C (2017) The STRING database in 2017: Quality-
825 controlled protein-protein association networks, made broadly accessible. *Nucleic Acids Res.* 45,
826 D362–D368. <https://doi.org/10.1093/nar/gkw937>

827 Tadesse T, Hewett EW, Nichols MA, Fisher KJ (2002) Changes in physicochemical attributes of
828 sweet pepper cv. Domino during fruit growth and development. *Scientia Horticulturae* 93(2):91-
829 103. doi: 10.1016/S0304-4238(01)00317-X

830 Tang W, Sun X, Yue J, Tang X, Jiao C, Yang Y, Niu X, Miao M, Zhang D, Huang S, Shi W, Li
831 M, Fang C, Fei Z, Liu Y (2019) Chromosome-scale genome assembly of kiwifruit *Actinidia*
832 *eriantha* with single-molecule sequencing and chromatin interaction mapping. *Giga Science* 8.
833 <https://doi.org/10.1093/gigascience/giz027>

834 Tang W, Zheng Y, Dong J, Yu J, Yue J, Liu F, Guo X, Huang S, Wisniewski M, Sun J, Niu X,
835 Ding J, Liu J, Fei Z, Liu Y (2016) Comprehensive transcriptome profiling reveals long noncoding
836 RNA expression and alternative splicing regulation during fruit development and ripening in
837 kiwifruit (*Actinidia chinensis*). *Front. Plant Sci.* 7. <https://doi.org/10.3389/fpls.2016.00335>

- 1 838 Untergasser A, Nijveen H, Rao X, Bisseling T, Geurts R, Leunissen JAM (2007) Primer3Plus, an
2 839 enhanced web interface to Primer3. *Nucleic Acids Res* 35. doi: 10.1093/nar/gkm306.
- 3 840 Vicente C, Mateos JL, Pedrosa MM, Legaz ME (1991) High-performance liquid chromatographic
4 841 determination of sugars and polyols in extracts of lichens and sugarcane juice. *Journal of*
5 842 *Chromatography*. 553, 271–283. [https://doi.org/10.1016/S0021-9673\(01\)88498-3](https://doi.org/10.1016/S0021-9673(01)88498-3)
- 6 843 Vieira M, Argenta L, Steffens C, Vieira A (2010) Postharvest quality preservation of “Bruno”
7 844 kiwifruit by ethylene control. *Revista Brasileira de Fruticultura* 32, 309–406.
8 845 <https://doi.org/10.1590/S0100-29452010000200008>
- 9 846 Wang T, Wang G, Jia ZH, Pan DL, Zhang JY, Guo ZR (2018) Transcriptome Analysis of
10 847 Kiwifruit in Response to *Pseudomonas syringae* pv. *actinidiae* Infection. *International journal of*
11 848 *molecular sciences* 19, 373. <https://doi.org/10.3390/ijms19020373>
- 12 849 Wang X, Ding Y, Wang Y, Pan L, Niu L, Lu Z, et al. (2017a) Genes involved in ethylene signal
13 850 transduction in peach (*Prunus persica*) and their expression profiles during fruit maturation.
14 851 *Scientia Horticulturae*. 224:306–16. <https://doi.org/10.1016/j.scienta.2017.06.035>.
- 15 852 Wang Y, Sugar D (2015) Postharvest Biology and Technology 1-MCP efficacy in extending
16 853 storage life of ‘Bartlett’ pears is affected by harvest maturity, production elevation, and holding
17 854 temperature during treatment delay. *Postharvest Biol. Technol.* 103, 1–8.
18 855 <https://doi.org/10.1016/j.postharvbio.2015.02.013>
- 19 856 Wang Z, Gerstein M, Snyder M (2009) RNA-Seq: A revolutionary tool for transcriptomics. *Nat.*
20 857 *Rev. Genet.* <https://doi.org/10.1038/nrg2484>
- 21 858 Wang Z, Liu Y, Li L, Li D, Zhang Q, Guo Y, Wang S, Zhong C, Huang H (2017b) Whole
22 859 transcriptome sequencing of *Pseudomonas syringae* pv. *actinidiae*-infected kiwifruit plants
23 860 reveals species-specific interaction between long non-coding RNA and coding genes. *Scientific*
24 861 *reports* 7, 4910. <https://doi.org/10.1038/s41598-017-05377-y>
- 25 862 Wills RBH (1998) Enhancement of senescence in non climacteric fruit and vegetables by low
26 863 ethylene levels. *Acta Hort.* 464, 159_/162.
- 27 864 Wu H, Ma T, Kang M, Ai F, Zhang J, Dong G, Liu J (2019) A high-quality *Actinidia chinensis*
28 865 (kiwifruit) genome. *Horticulture Research* 6, 117. <https://doi.org/10.1038/s41438-019-0202-y>
- 29 866 Xu X, Yin L, Ying Q, Song H, Xue D, et al. (2013) High-Throughput Sequencing and Degradome
30 867 Analysis Identify miRNAs and Their Targets Involved in Fruit Senescence of *Fragaria ananassa*.
31 868 *PLOS ONE* 8(8): e70959. <https://doi.org/10.1371/journal.pone.0070959>
- 32 869 Xu ZC, Hyodo H, Ikoma Y, Yano M, Ogawa K (2000) Relation between ethylene-producing
33 870 potential and gene expression of 1-aminocyclopropane-1-carboxylic acid synthase in *Actinidia*
34 871 *chinensis* and *A. deliciosa* fruits. *J. Japanese Soc. Hortic. Sci.* 69, 192–194.
35 872 <https://doi.org/10.2503/jjshs.69.192>
- 36 873 Xu ZC, Ikoma Y, Yano M, Ogawa K, Hyodo H (1998) Varietal differences in the potential to
37 874 produce ethylene and gene expression of ACC synthase and ACC oxidase between “Kui mi” and
38 875 “Hong xin” of Chinese kiwifruit. *J. Japanese Soc. Hortic. Sci.* 67, 204–209.
39 876 <https://doi.org/10.2503/jjshs.67.204>
- 40
41
42
43
44
45
46
47
48
49
50
51
52
53
54
55
56
57
58
59
60
61
62
63
64
65

877 Zhang A, Wang W, Tong Y, Li M, Grierson D, Ferguson I, Chen K, Yin X (2018) Transcriptome
878 Analysis Identifies a Zinc Finger Protein Regulating Starch Degradation in Kiwifruit. *Plant*
879 *Physiology* 178, 850 LP – 863. <https://doi.org/10.1104/pp.18.00427>

880 Zhang L, Li S, Liu X, Song C, Liu X (2012) Postharvest Biology and Technology Effects of
881 ethephon on physicochemical and quality properties of kiwifruit during ripening. *Postharvest*
882 *Biol. Technol.* 65, 69–75. <https://doi.org/10.1016/j.postharvbio.2011.11.004>

883 Zhou Z, Cong P, Tian Y, Zhu Y (2017) Using RNA-seq data to select reference genes for
884 normalizing gene expression in apple roots. *PLoS One* 12, 1–17.
885 <https://doi.org/10.1371/journal.pone.0185288>

886 Ziliotto F, Begheldo M, Rasori A, Bonghi C, Tonutti P (2008) Transcriptome profiling of ripening
887 nectarine (*Prunus persica* L. Batsch) fruit treated with 1-MCP. *J. Exp. Bot.* 59, 2781–2791.
888 <https://doi.org/10.1093/jxb/ern136>

889 Zou J, Chen J, Tang N, Gao Y, Hong M, Wei W, Cao H, Jian W, Li N, Deng W, Li Z (2018)
890 Transcriptome analysis of aroma volatile metabolism change in tomato (*Solanum lycopersicum*)
891 fruit under different storage temperatures and 1-MCP treatment. *Postharvest Biol. Technol.* 135,
892 57–67. <https://doi.org/10.1016/j.postharvbio.2017.08.017>

893

894 TABLE AND FIGURE LEGENDS

895 **Table 1.** Summary of alignment results of filtered reads per treatment (not treated fruit, T0;
896 1-MCP, T1; and Ethrel®, T2) and day (D4 and D13).

897 **Fig. 1.** Fruit chlorophyll (Skin I_{AD} and Flesh I_{AD}), flesh color (L^*), and soluble solids
898 content (%) changes in ‘Hayward’ kiwifruit during 29 d of storage at 20 °C at two ripeness
899 stages (E1 and E2) and four postharvest periods: day 0 (at harvest), day 1 (48 h after
900 harvest), day 15 (after 15 days) and day 29 (after 29 days). In red (not treated fruit), blue
901 (1-MCP), and purple (Ethrel®) are shown. Standard error of each treatment and day is
902 shown and significant differences between treatments per day are shown by Tukey test
903 at p-value < 0.05.

904 **Fig. 2.** CO₂ emissions (ml kg⁻¹ h⁻¹) of ‘Hayward’ kiwifruit during 29 d of storage at 20
905 °C at two ripeness stages (E1 and E2). In red (not treated fruit), blue (1-MCP), and purple

1
2
3
4
5
6
7
8
9
10
11
12
13
14
15
16
17
18
19
20
21
22
23
24
25
26
27
28
29
30
31
32
33
34
35
36
37
38
39
40
41
42
43
44
45
46
47
48
49
50
51
52
53
54
55
56
57
58
59
60
61
62
63
64
65

906 (Ethrel®). Standard error of each treatment and day is shown and significant differences
907 between treatments per day are shown by Tukey test at p-value < 0.05.

908 **Fig. 3.** Changes in fruit firmness (P7.9), flesh firmness (P2), and core firmness (P2) in
909 ‘Hayward’ kiwifruit during 29 d of storage at 20 °C at two ripeness stages (E1 and E2).
910 In red (not treated fruit), blue (1-MCP), and purple (Ethrel®). Standard error of each
911 treatment and day is shown and significant differences between treatments per day are
912 shown by Tukey test at p-value < 0.05.

913 **Fig. 4.** Principal component analysis (PCA), including all evaluated traits per treatment
914 (above: T0, not treated fruit; T1, 1-MCP; and T2, Ethrel®) and time (below: A, day 1; B,
915 day 15; and C, day 29).

916 **Fig. 5.** a) Number of DEGs by FPKM range in ‘Hayward’ kiwifruit between treatments
917 (T0, not treated fruit; T1, 1-MCP; and T2, Ethrel®) and days (D4 and D13) including
918 18,036 DEGs at p-value < 0.005. b) Number of up- and downregulation genes with a
919 differential expression of at least double in day 4 and day 13 for each treatment
920 comparison (T0vsT1, T0vsT2, and T1vsT2).

921 **Fig. 6.** Functional enrichment analysis performed for all DEGs in kiwifruit with the
922 BiNGO plug-in in Cytoscape. Functional enrichment analysis performed for all DEGs in
923 kiwifruit under the different treatments (T0, not treated fruit; T1, 1-MCP; and T2,
924 Ethrel®), for day 4 (D4) and day 13 (D13), with the BiNGO complement in Cytoscape.
925 Venn diagrams (A and E) are showing the number of DEGs while the assigned GO terms
926 were used to classify the functions of the DEGs according to biological processes (B and
927 F), cellular components (C and G) and molecular functions (D and H). The colors on the
928 edges of the nodes represents the p-value, as shown by the legend in the graph.

1
2
3
4
5
6
7
8
9
10
11
12
13
14
15
16
17
18
19
20
21
22
23
24
25
26
27
28
29
30
31
32
33
34
35
36
37
38
39
40
41
42
43
44
45
46
47
48
49
50
51
52
53
54
55
56
57
58
59
60
61
62
63
64
65

929 **Fig. 7.** KEGG pathway analysis of DEGs. Bubble chart shows the enrichment of DEGs
930 in the signaling pathways. The y-axis label represents the pathways, and the x-axis label
931 represents the rich factor. The size of the bubble represents the amount of DEGs enriched,
932 and the color shows the Q value to each pathway.

933 **Fig. 8.** DEGs' IPP network. The network is showing the protein-protein interaction nodes.
934 The size of the node is proportional to the number of genes that interact with proteins,
935 and the color of the node represents each pathway. The colors on the edges of the nodes
936 represents the p-value, as shown by the legend in the graph.

937 **Fig. 9.** Summary of the top hit genes up and down-regulated considering not treated fruit
938 (T0) and contrasting treatments (T1, 1-MCP vs T2, Ethrel®) in the main pathways
939 involved. Red color indicates a minimum value of FPKM while light yellow indicates a
940 maximum FPKM.

941 **Fig. 10.** The expression levels of the genes revealed by RT-qPCR and RNA-seq. In each
942 panel, the post treatment days (day 4 and day 13) are indicated, where the bars arranged
943 from left to right represent the treatments (T0, not treated fruit; T1, 1-MCP; and T2,
944 Ethrel®) to which the kiwifruit were subjected. The annotation of the selected genes are
945 as follows: Achn069361: NYC (porphyrin and chlorophyll); Achn218701: ATSPS4F
946 (starch and sucrose); Achn271251: CHLM (porphyrin and chlorophyll); Achn152281:
947 ACO3 (citrate and glycosylate); Achn219321: PDC2 (glycolysis and gluconeogenesis);
948 Achn281901: PPa1 (oxidative phosphorylation); Achn051381: EC: 3.2.1.15 (pentose and
949 glucuronate); Achn253411: EC: 2.7.1.159 2.7.1.134 (inositol phosphate); Achn358091:
950 PRF3 (actin cytoskeleton); Achn163471: POR (porphyrin and chlorophyll);
951 Achn383491: EC 6.1.1.17 (porphyrin and chlorophyll); Achn330311: ATPME3 (pentose
952 and glucuronate); Achn328501: CRD1 (porphyrin and chlorophyll); Achn372361: APL3
953 (starch and sucrose); and Achn282431: EC: 1.5.3.1 1.5.3.7 (lysine degradation).

1
2
3
4
5
6
7
8
9
10
11
12
13
14
15
16
17
18
19
20
21
22
23
24
25
26
27
28
29
30
31
32
33
34
35
36
37
38
39
40
41
42
43
44
45
46
47
48
49
50
51
52
53
54
55
56
57
58
59
60
61
62
63
64
65

954 Achn005971 (AGB1) and Achn107351 (ACTIN 7) were used as the reference genes. The
955 error bars in each column indicate the SD of two replicates. The different asterisks in the
956 bars indicate statistically significant differences with a $P < 0.05$ (unidirectional ANOVA,
957 Tukey tests).

958 SUPPLEMENTARY MATERIAL

959 **Fig. S1.** Fructose, glucose, and ascorbic acid content by treatment (not treated fruit, T0;
960 1-MCP, T1; and Ethrel®, T2) and days (D1, D15 and D29). Standard error of each
961 treatment and day is shown. Significant differences between fructose and glucose
962 (above) per day and treatment and significant differences for ascorbic acid content
963 (below) between treatments for each day are shown by Tukey test at p -value < 0.05 .

964 **Fig. S2.** Principal components analysis (PCA) of the RNA-seq for each treatment (not
965 treated fruit, T0; 1-MCP, T1; and Ethrel®, T2) and day (D4 and D13).

966 **Fig. S3.** Quantity versus dispersion of the genes for each treatment (not treated fruit, T0;
967 1-MCP, T1; and Ethrel®, T2) and day (D4 and D13).

968 **Fig. S4.** Gene density for each treatment (not treated fruit, T0; 1-MCP, T1; and Ethrel®,
969 T2) and day (D4 and D13). Average values (left), and including the three biological
970 replicates (right), per each condition.

971 **Fig. S5.** Dispersion diagrams for identifying global changes and trends in gene expression
972 among treatments (not treated fruit, T0; 1-MCP, T1; and Ethrel®, T2) and days (D4 and
973 D13).

974 **Fig. S6.** Boxplots of fragments per kilobase million (FPKM) for each treatment (not
975 treated fruit, T0; 1-MCP, T1; and Ethrel®, T2) and day (D4 and D13). Average values
976 (left), and including the three biological replicates (right), per each condition.

977 **Fig. S7.** Volcano plots of the significant relationship between \log_{10} (p -value) and
978 \log_2 (fold change) for each treatment (not treated fruit, T0; 1-MCP, T1; and Ethrel®, T2)

1
2
3
4
5
6
7
8
9
10
11
12
13
14
15
16
17
18
19
20
21
22
23
24
25
26
27
28
29
30
31
32
33
34
35
36
37
38
39
40
41
42
43
44
45
46
47
48
49
50
51
52
53
54
55
56
57
58
59
60
61
62
63
64
65

979 and day (D4 and D13). This graph defines the genes' significant cutoff points (alpha value
980 or p-value). In this case, the alpha is fixed at 0.005, obtaining 18,036 DEGs from a total
981 of 79,614 genes. The non-significant genes are shown in black, and the significant genes
982 are shown in red.
983
984 **Fig. S8.** Number of genes by count range for each treatment (not treated fruit, T0; 1-MCP,
985 T1; and Ethrel®, T2) and day (D4 on the left, and D13 on the right).
986 **Fig. S9.** Pentose phosphate KEGG pathway.
987 **Fig. S10.** Citrate cycle (TCA cycle) KEGG pathway.
988 **Fig. S11.** Glycolysis-Gluconeogenesis KEGG pathway.
989 **Fig. S12.** Starch and sucrose metabolism KEGG pathway.
990 **Fig. S13.** Pentose phosphate KEGG pathway.
991 **Fig. S14.** Porphyrin and chlorophyll metabolism KEGG pathway.
992 **Fig. S15.** Plant hormone signal transduction KEGG pathway.
993 **Fig. S16.** Carotenoid biosynthesis KEGG pathway.
994 **Table. S1.** Summary of evaluated traits for ripeness stage 1 at harvest.
995 **Table. S2.** Summary of evaluated traits for ripeness stage 2 at harvest.
996 **Table. S3.** Pearson correlations of ripeness stage 1.
997 **Table. S4.** Pearson correlations of ripeness stage 2.
998 **Table. S5.** BLUP coefficients for both ripeness stages.
999 **Table. S6.** Raw data RNA-seq statistics.
1000 **Table. S7.** Total filtered reads and alignment results by replicate.
1001 **Table. S8.** Test genes in different treatments and days.xlsx
1002 **Table. S9.** Gene Ontology_Bingo.xlsx
1003 **Table. S10.** Analysis of enrichment of pathways_Kegg.xls

1004 **Table. S11.** PPI string_1mcp.xlsx

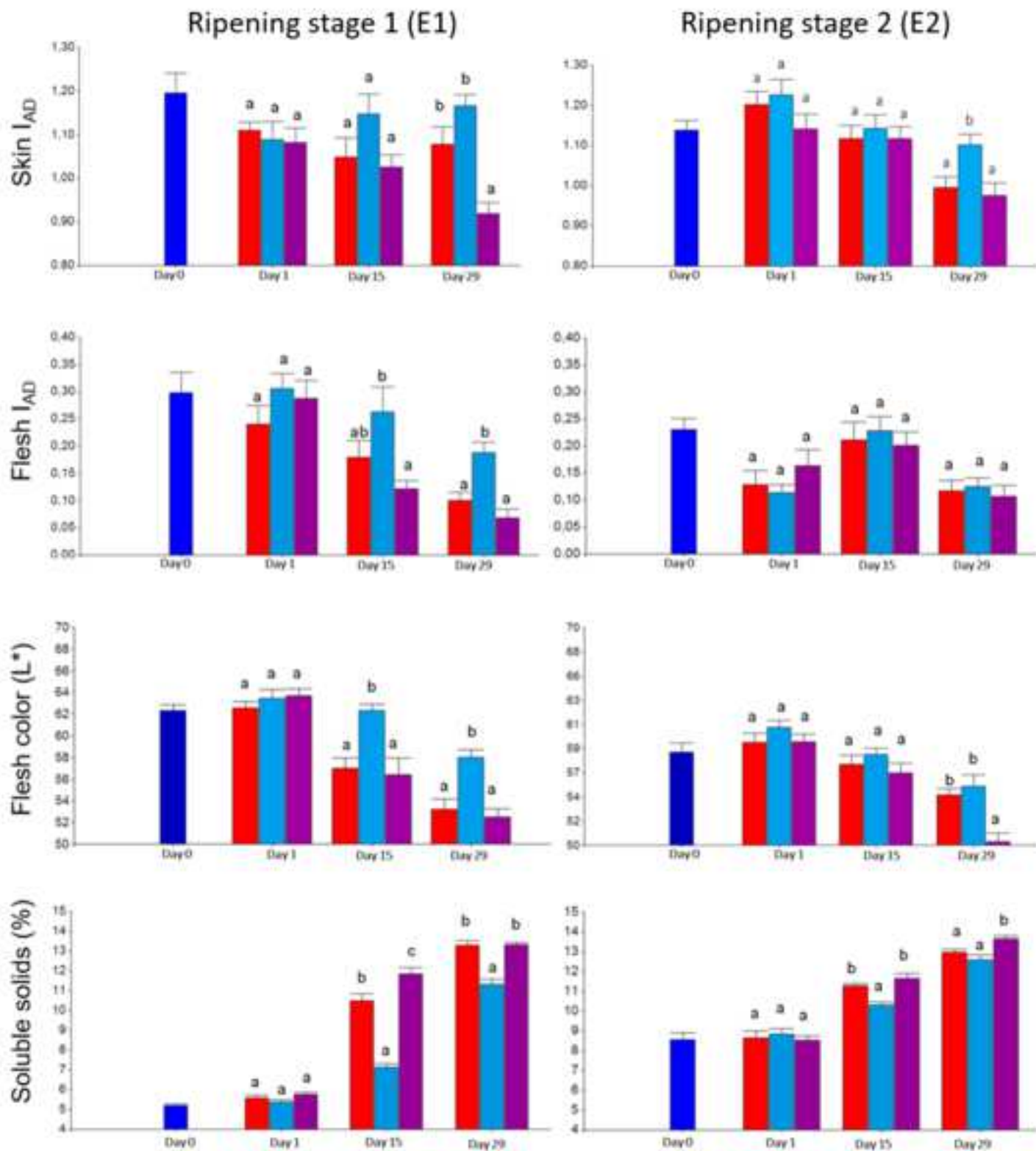
1
2
3
4
5
6
7
8
9
10
11
12
13
14
15
16
17
18
19
20
21
22
23
24
25
26
27
28
29
30
31
32
33
34
35
36
37
38
39
40
41
42
43
44
45
46
47
48
49
50
51
52
53
54
55
56
57
58
59
60
61
62
63
64
65

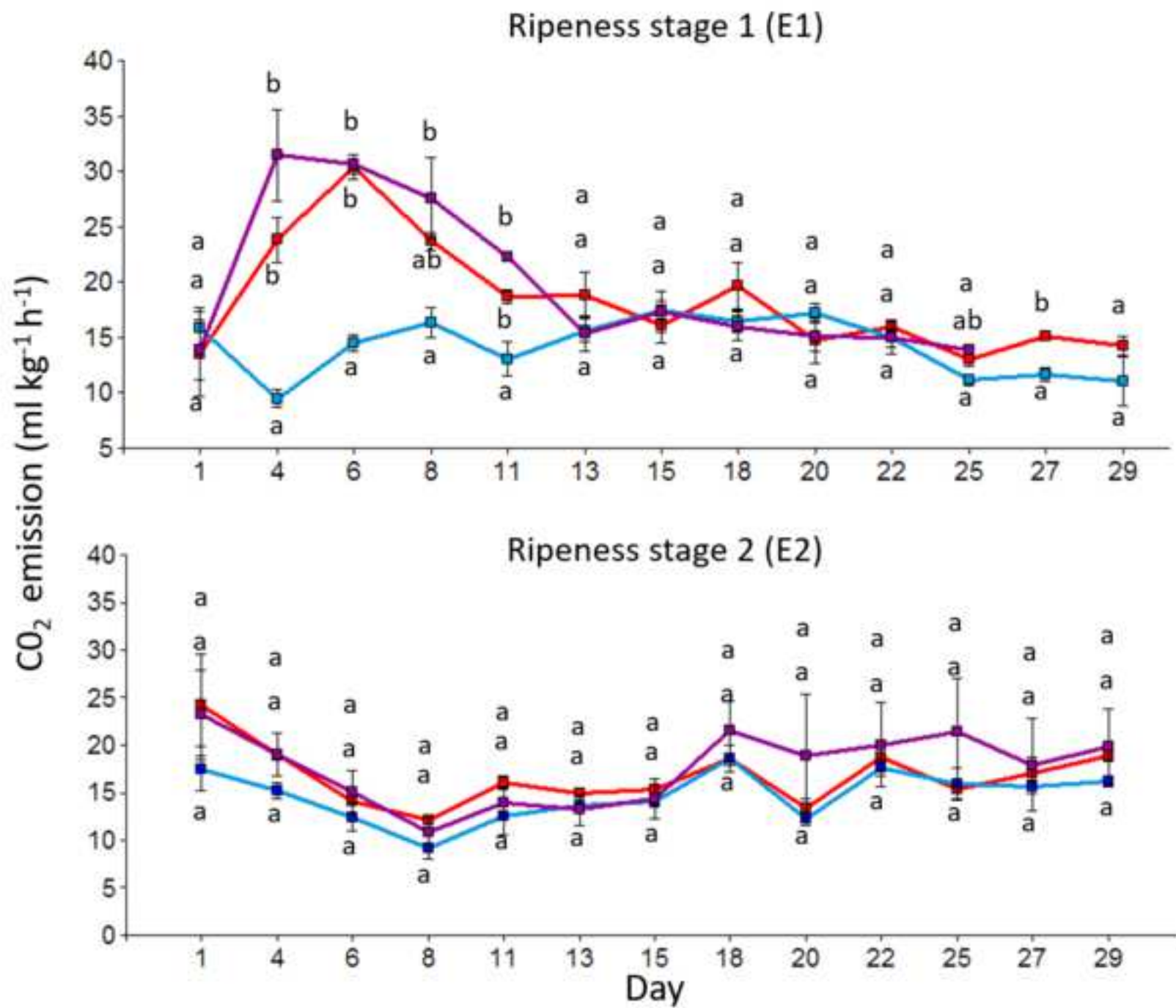
1005 **Table. S12.** RT-qPCR.xlsx

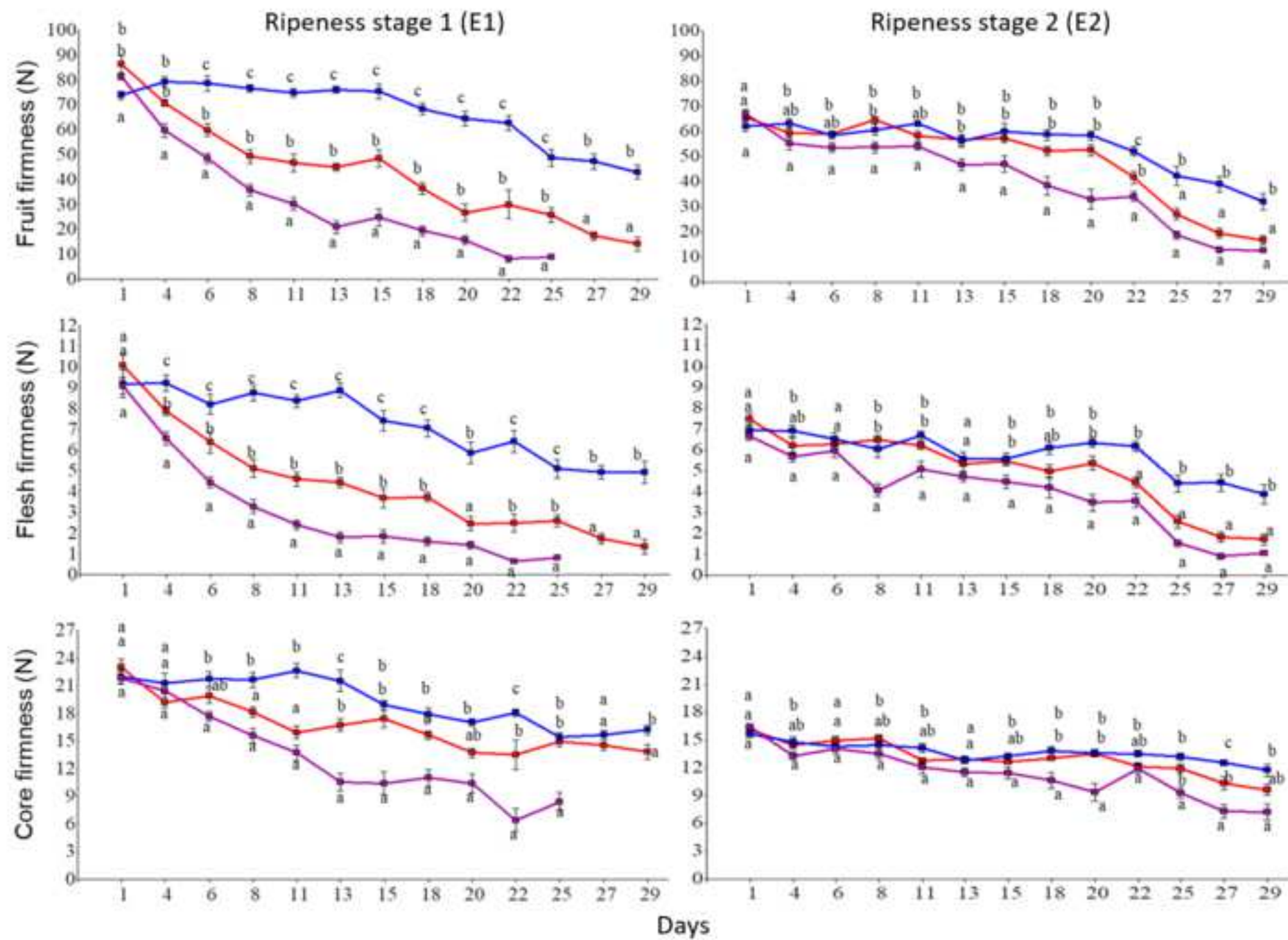
Table 1. Summary of alignment results of filtered reads per treatment (not treated fruit, T0; 1-MCP, T1; and Ethrel®, T2) and day (D4 and D13).

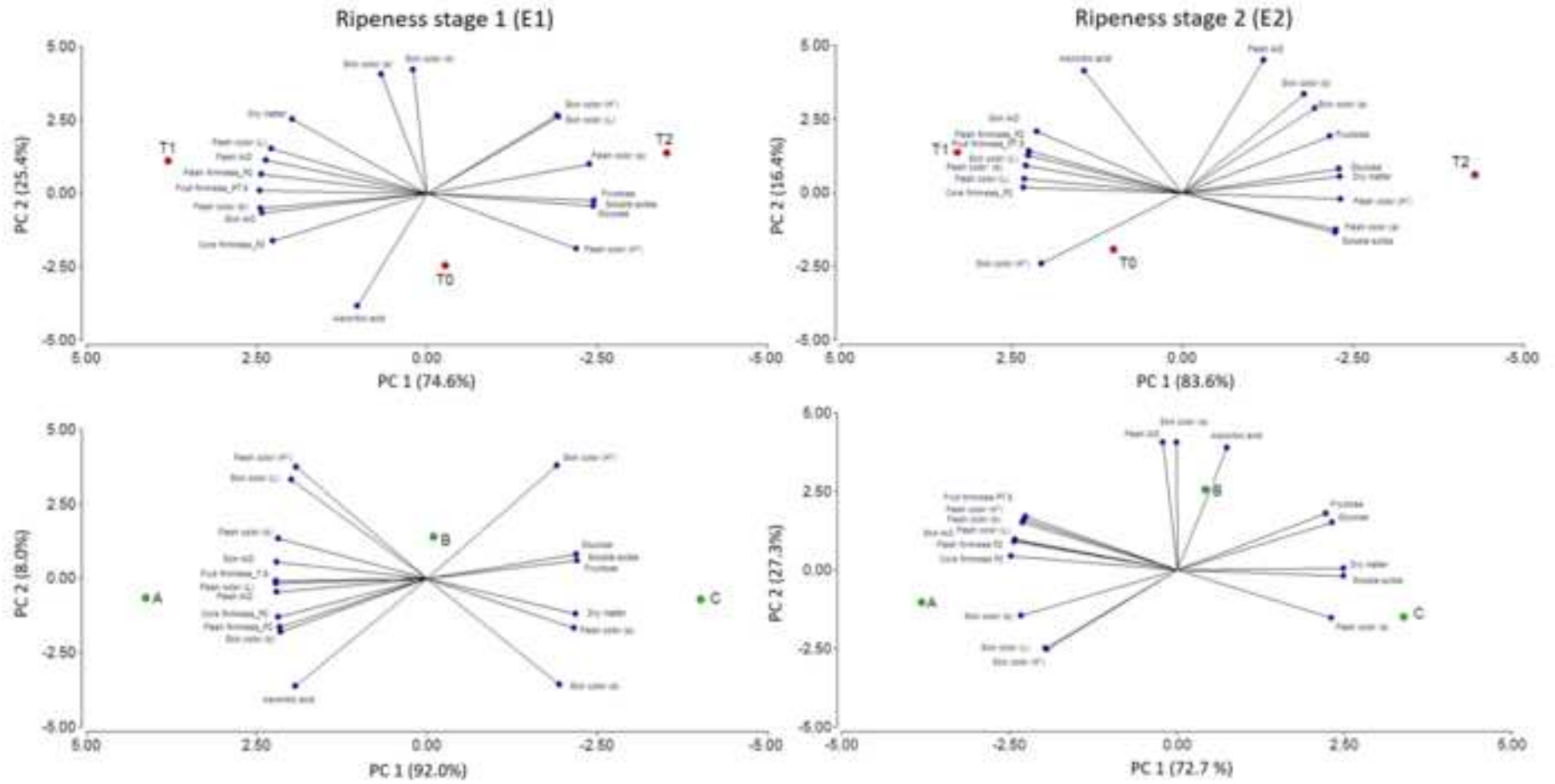
ID*	Filtered reads	Reads not aligned	Reads (=1)	Reads >1	Reads aligned
T0_D4	17,428,301	5,077,644	6,295,065	6,055,592	12,350,657
T1_D4	17,807,074	5,085,540	6,546,095	6,175,439	12,721,534
T2_D4	16,956,703	4,742,136	6,119,174	6,095,393	12,214,567
T0_D13	16,972,564	5,101,475	6,007,613	5,863,476	11,871,089
T1_D13	17,073,064	5,058,979	6,095,167	5,918,918	12,014,085
T2_D13	18,941,593	5,729,116	6,685,738	6,526,738	13,212,476
Average	17,529,883 (100%)	5,132,482 (29.3%)	6,291,475 (35.9%)	6,105,926 (34.8%)	12,397,401 (70.7%)

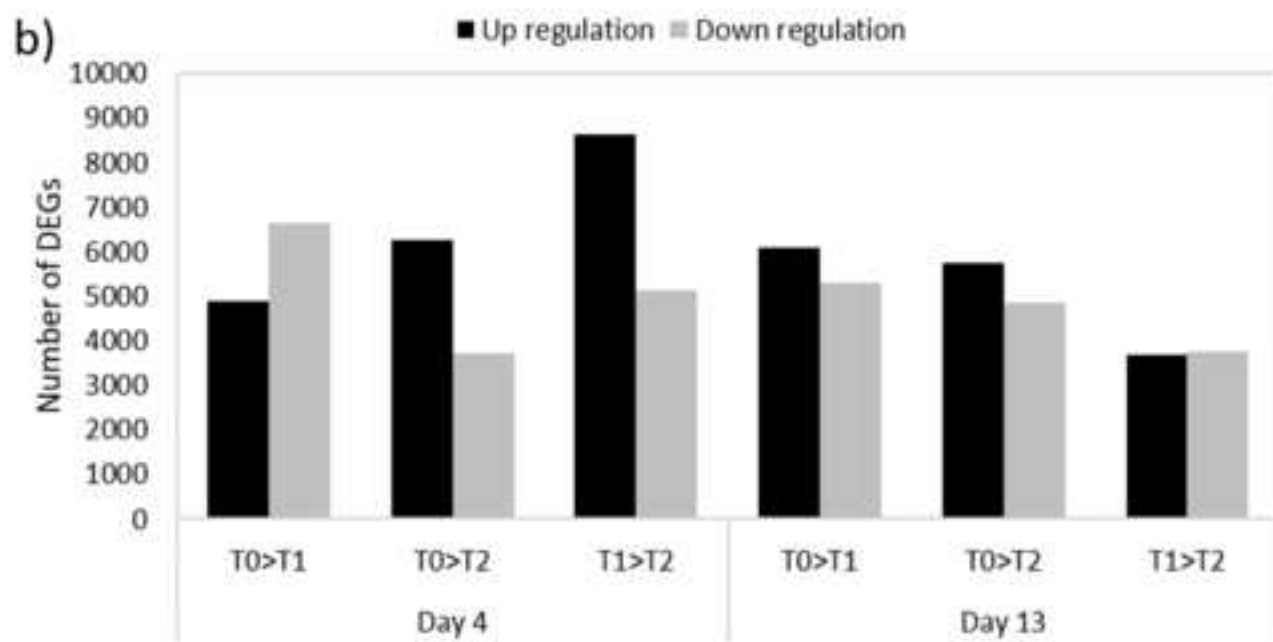
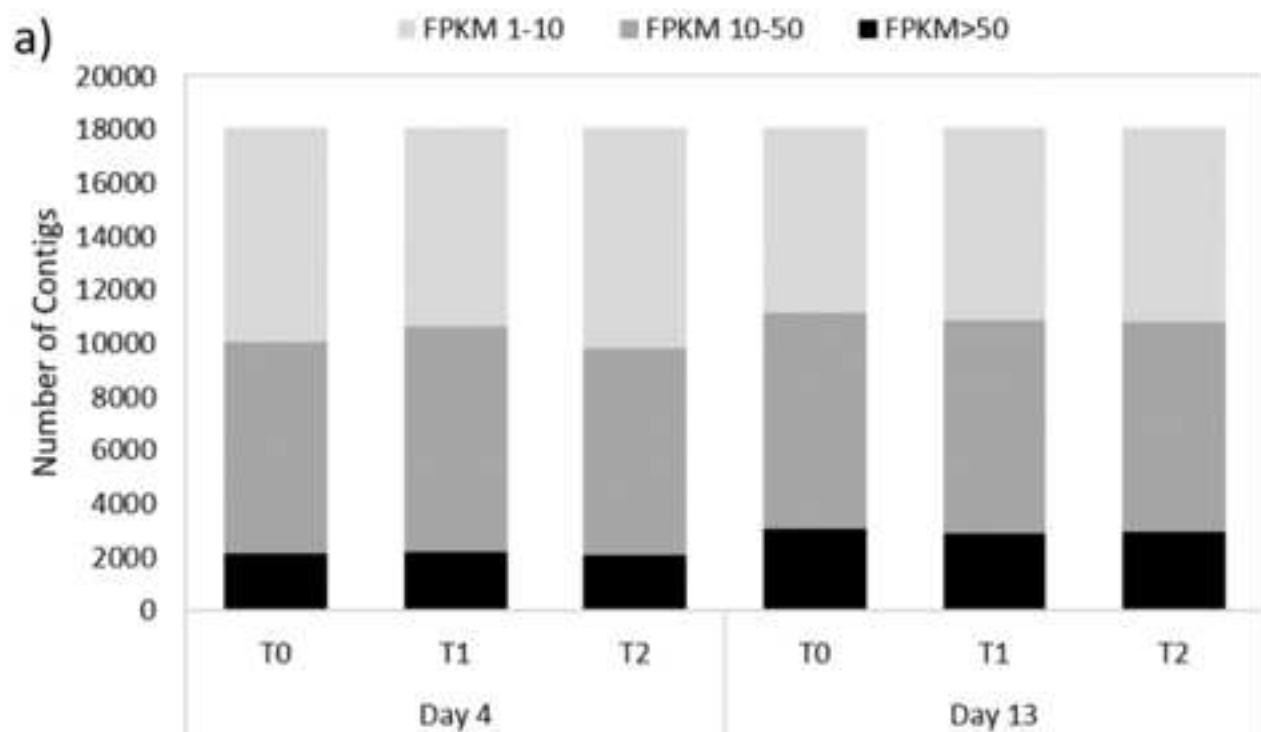
Data for each treatment and day are from three biological replicates (*). Reads aligned to unique position (=1) and reads aligned to multiple positions (<1)









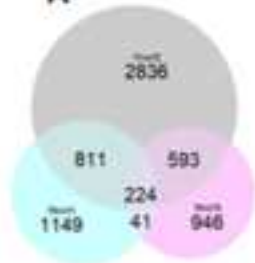


D4)

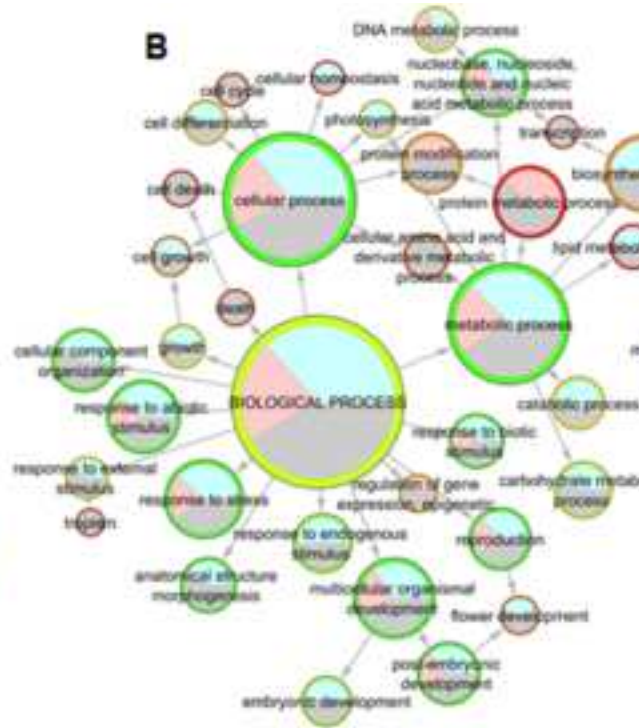
Symbology:

- T0vsT1
- T0vsT2
- T1vsT2

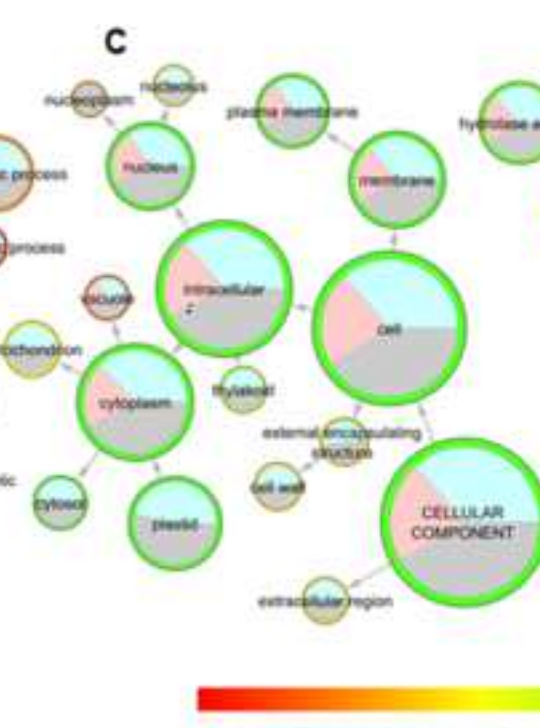
A



B



C



D

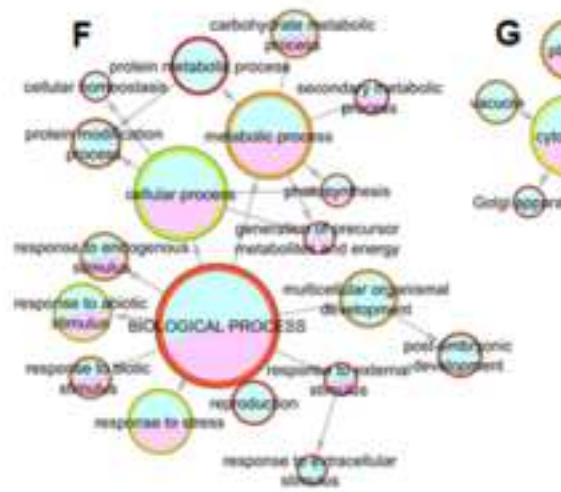


D13)

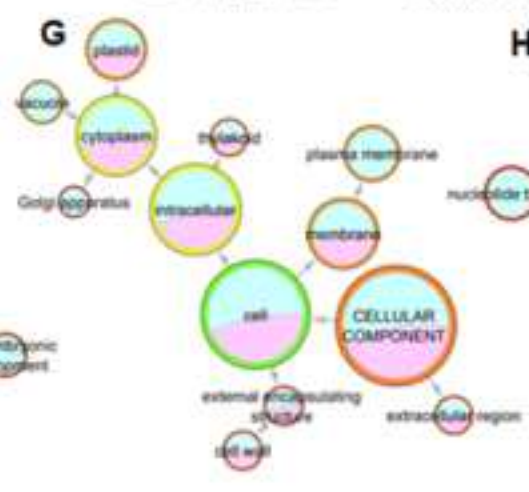
E



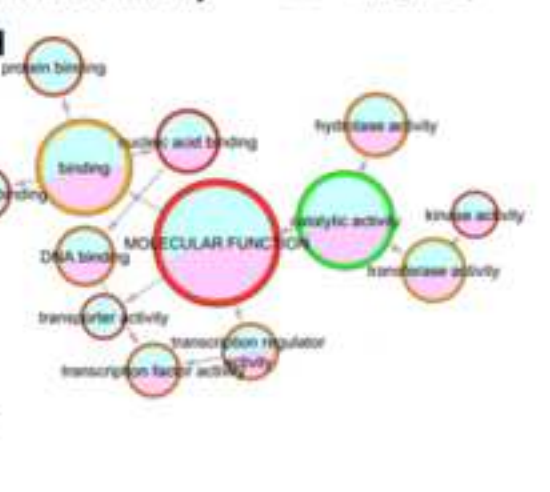
F



G



H



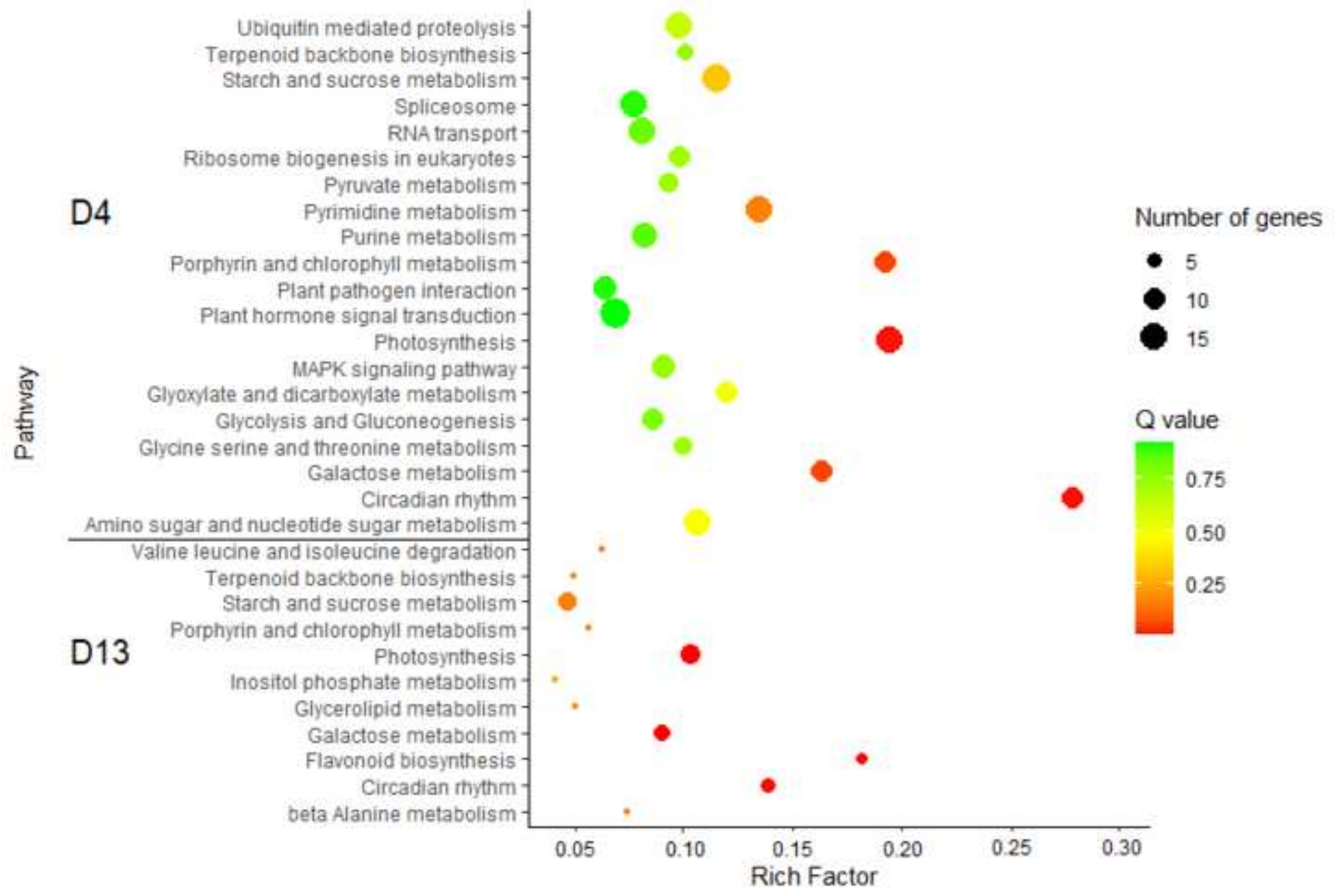
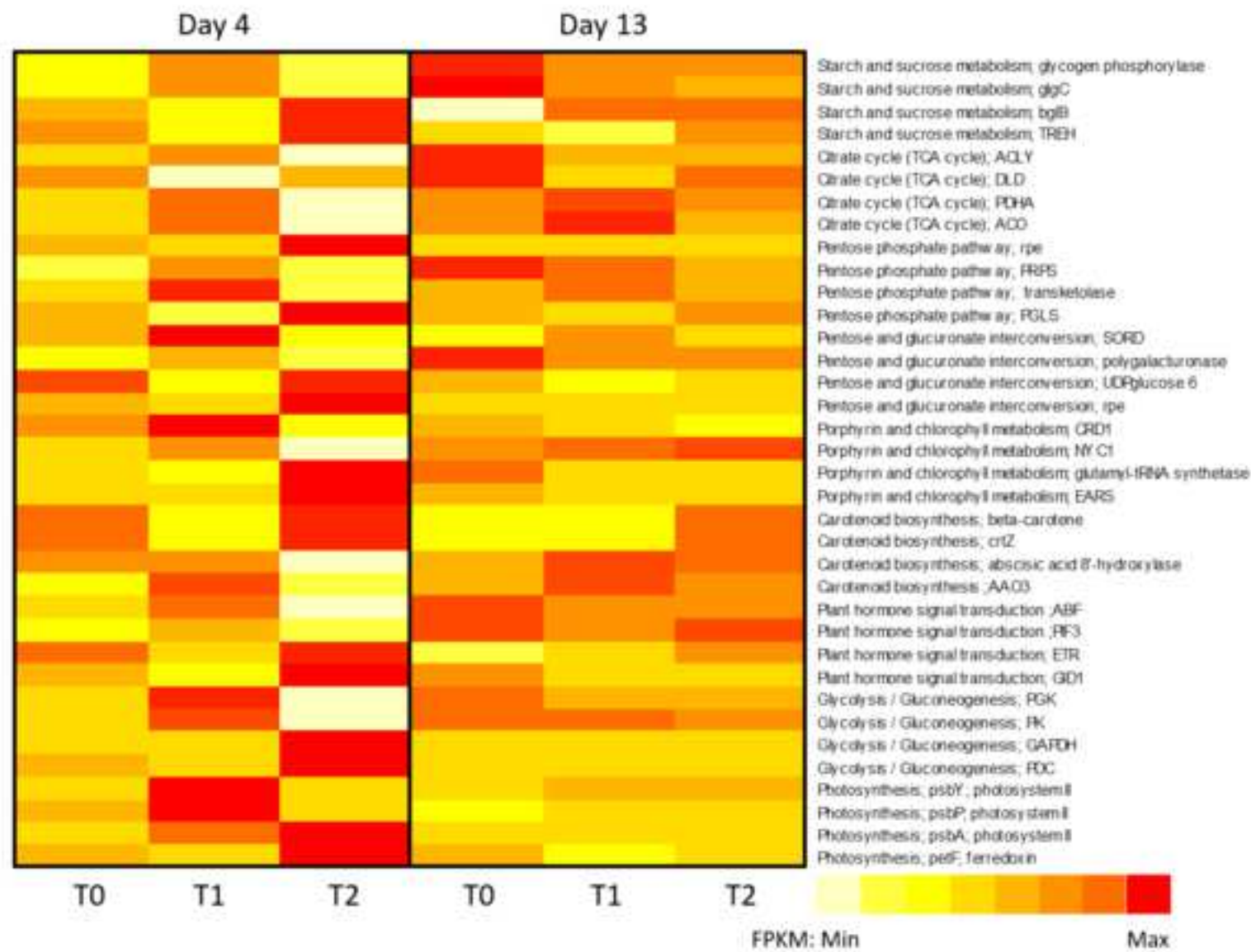
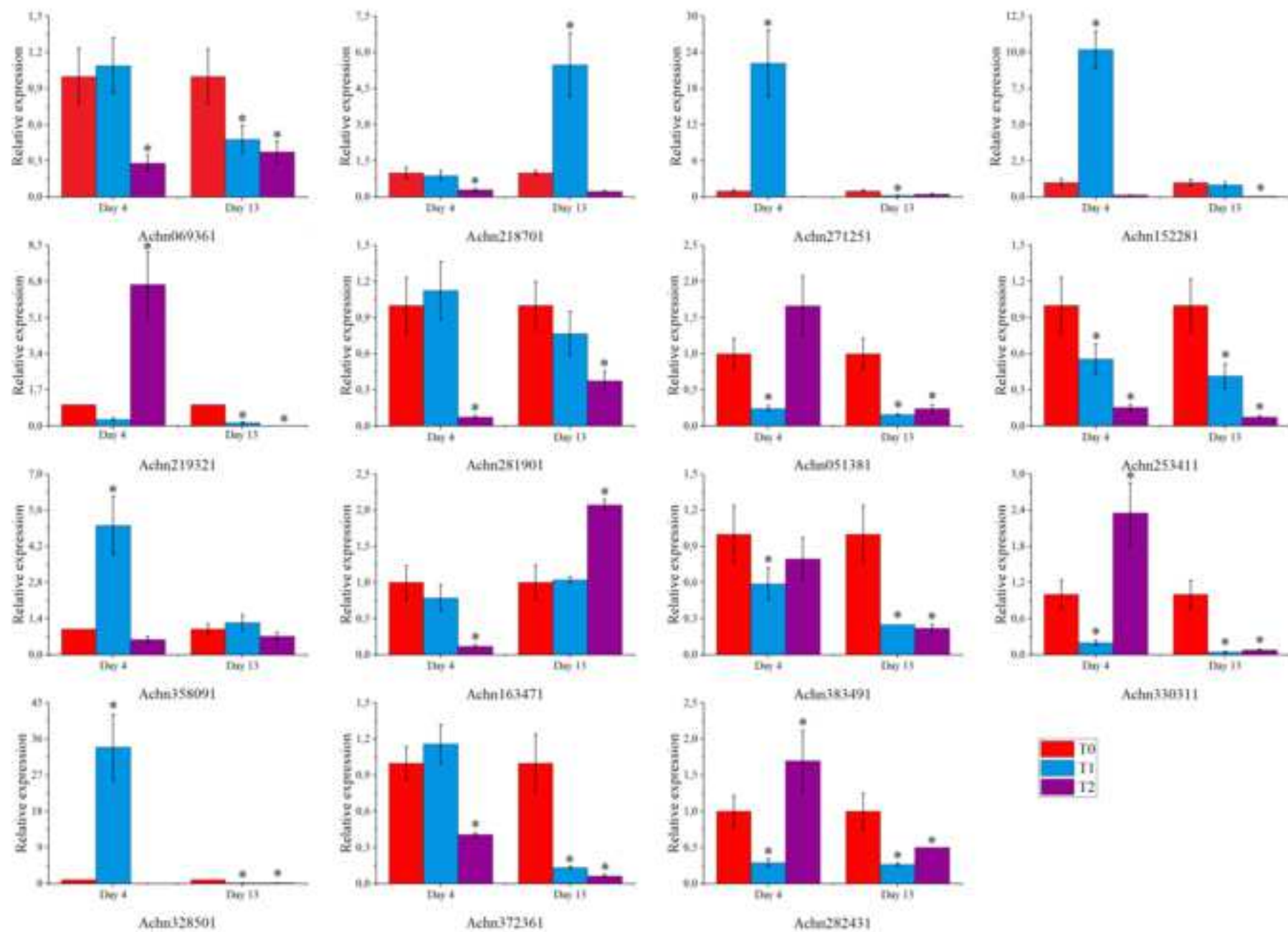




Fig. 9



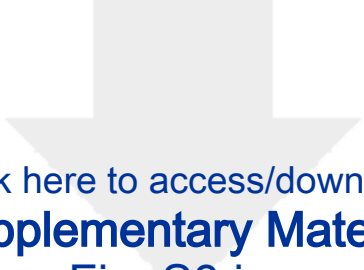




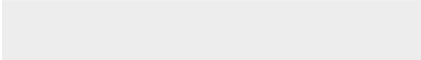

Click here to access/download
Supplementary Material
Fig. S1.png




Click here to access/download
Supplementary Material
Fig. S2.png




Click here to access/download
Supplementary Material
Fig. S3.jpg







Click here to access/download
Supplementary Material
Fig. S4.jpg





Click here to access/download
Supplementary Material
Fig. S5.jpg

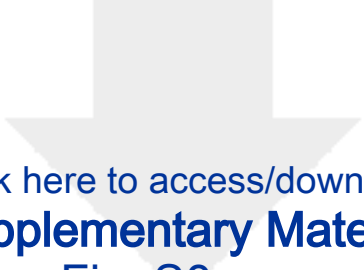




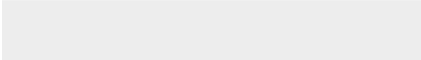

Click here to access/download
Supplementary Material
Fig. S6.png




Click here to access/download
Supplementary Material
Fig. S7.jpg



Click here to access/download
Supplementary Material
Fig. S8.png



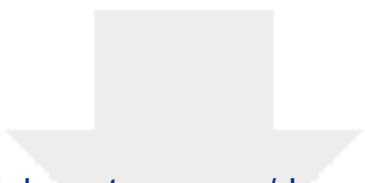


Click here to access/download
Supplementary Material
Fig. S9.png




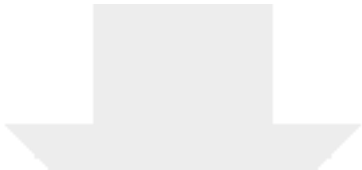
Click here to access/download
Supplementary Material
Fig. S10.png



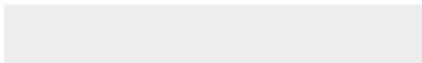
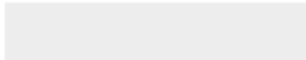


Click here to access/download
Supplementary Material
Fig. S11.png





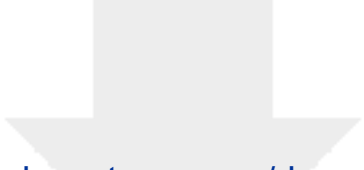
Click here to access/download
Supplementary Material
Fig. S12.jpeg



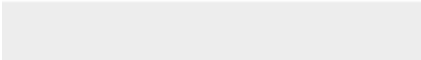



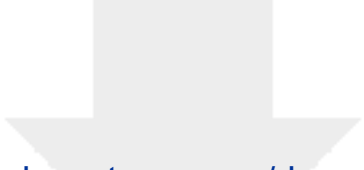
Click here to access/download
Supplementary Material
Fig. S13.png



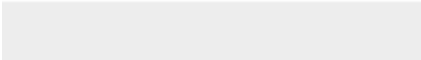



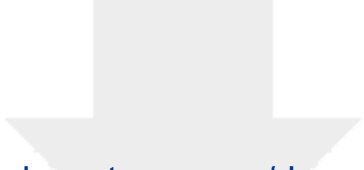
Click here to access/download
Supplementary Material
Fig. S14.jpeg



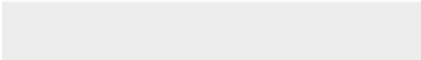



Click here to access/download
Supplementary Material
Fig. S15.jpeg



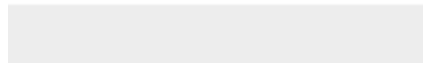



Click here to access/download
Supplementary Material
Fig. S16.jpeg





Click here to access/download
Supplementary Material
Supplementary Tables S1-S7.docx





Click here to access/download

Supplementary Material

Table S8. Test genes in different treatments and days..xlsx



[Click here to access/download](#)

Supplementary Material

Table S9. Gene Ontology_Bingo.xlsx

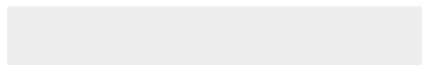




[Click here to access/download](#)

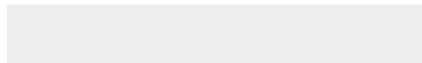
Supplementary Material

Table S10. Analysis of enrichment of pathways_Kegg.xls





Click here to access/download
Supplementary Material
Table S11. PPI string_1mcp.xlsx





Click here to access/download
Supplementary Material
Table S12. RT-qPCR.xlsx

Comments for the Author:

AE: The manuscript requires minor revisions but is overall a good quality manuscript fitting the scope of TGGE, it could be published after corrections following the reviewers' recommendations, below.

Reviewer #1: The present work is interesting as it investigates the main protagonists of the ripening of kiwifruits in the post-harvesting steps. It is a very big and complex work that I really appreciated. Thus, I have only some minor suggestions for the authors to improve their paper:

a) the title should be revised because unclear.

The title was modified for: "Transcriptome analysis and postharvest behavior of the kiwifruit 'Actinidia deliciosa' reveal the role of ethylene-related phytohormones during fruit ripening"

b) in the abstract what are 1-MCP and Ethrel should be reported.

In the Abstract section, 1-MCP and Ethrel® treatments have been specified as ethylene inhibitor and ethylene stimulator respectively (lines: 32-33)

c) how was identified the plant genetic identify at variety level?

The 'Hayward' variety identity was corroborated through "Viveros Biotecnia" in an orchard in Teno (line 154)

d) No citation is reported for the methods applied to measure vitamin C content, sugar content, etc. Please, add them.

Methodology references for sugar measurements (Vicente et al., 1991) and for vitamin C content (El Gindy et al., 2006) were cited (lines 196 and 201).

e) Why did not the authors consider RNA smaller than 100 bp? It could be interesting to also investigate presence and variation of microRNA that recently have been documented to possess a key role in the determination of plant development. I strongly suggest the authors to make a further study, in future, and recover the data of the small RNAs from their libraries and check putative differences and microRNAs with potential function in kiwifruit ripening. In the present paper, thus, they should state that also microRNA could have an important activity in regulating kiwifruit maturation and that it could be investigated. In particular, they should also underline the role that plant microRNA could also have on the consumers of these fruits. I suggest to read and cite some papers to support this evidence: Journal of experimental botany, 2013, 64.7: 1863-1878;. Scientific reports, 2019, 9.1: 1-14; PLoS One, 2013, 8.8: e70959.

I agree, in the following studies we will consider this fact and we will recovery small RNAs in order to find evidence about how this small RNA is affecting ripening in kiwifruit. In addition, as you have suggested we have cited the papers above (Karlova et al., 2013 in Journal of Experimental Botany and Xu et al., 2013 in PLOS ONE) in the discussion section, considering further analysis using small RNA (lines: 620-621).

f) line 281 (and others) I do not understand the meaning of the symbol reported as a full stop in "10 $\mu\text{mol} * \text{L}^{-1}$ ". Please, remove it.

This symbol was removed (new lines 283 and 284). Therefore, " $\mu\text{mol} * \text{L}^{-1}$ " was replaced by " $\mu\text{mol} \text{L}^{-1}$ "

g) The patronymic of all cited plant species should be reported. Moreover, the scientific names of plants should be reported in italics (even in reference list).

The patronymic of all plant species was cited (lines: 92-95) and plant scientific names have been reported in italics even in the reference list

Reviewer #2: The several gene networks related to kiwifruit ripening were found after treatments by 1-mcp and Ethrel, and the author also verified the gene expression by qRT-PCR analysis. These results provide some important reference information for extending the shelf-life of kiwifruit using 1-MCP and Ethrel. The grammar is also good.

(1) In the section of plant materials, genus and species names of kiwifruit are required.

In this section and in all manuscript genus and species names of kiwifruit and other species were added.

(2) In the section of discussion, the things discussed are not very clear. It is better divided into several subsections.

This section was divided in several subsections as follows: fruit phenotyping (line 476), sequencing and alignment results (line 501), differentially expressed genes (DEGs) and functional annotation (line 516), Protein-protein interaction network of DEGs and related pathways (line 534)

Reviewer #3: In their manuscript "Postharvest behavior and the expression of 1-MCP and ethylene responses in genes of the kiwifruit 'Actinidia deliciosa' during ripening", Juan Salazar and colleagues analyze the effect of 1-MCP and Ethrel® treatment on the kiwifruit at the physiological and molecular level. First the authors analyzed different parameters (chlorophyll and sugar content, CO₂ emission, firmness...) at different time points (0, 1, 15 and 29 days after harvesting) after mock, 1-MCP or Ethrel® treatment made at two different ripeness stages (5.2% (E1) and 8.0% (E2) soluble sugar content) to evaluate the effect of the treatment on fruit ripening and post-harvest behavior. As expected, 1-MCP (ethylene biosynthesis inhibitor) and Ethrel® (climacteric fruit ripening accelerator) treatments led to

opposite effects, with delay and accelerated ripening respectively (reported by changes of chlorophyll content, fruit flesh color and firmness, and increase of soluble sugar concentration), compared to mock treatment. Their analyses revealing a bigger effect in the E1 condition and the biggest differences being at 4 days (burst of respiration rate) and 13 days (highest fruit firmness difference) they carried out a RNAseq analysis on fruits in the different conditions at these two stages. RNAseq analyses revealed as expected a high number of differentially expressed genes with many genes involved in the central carbon and chlorophyll metabolism in relation with the timing difference in the chlorophyll degradation and fruit ripening between the treatments. Taken together, these data provides a very complete description of the role of ethylene in kiwifruit ripening at a physiological and gene expression level and will be of great interest to the scientific community. However I think that the manuscript could be improved and I address my concerns in several comments below. I hope that my comments are constructively contributing to improve the quality of the manuscript. In my opinion, the manuscript is suitable for publication in TGGE, after the authors have addressed the following comments and questions:

Scientific concerns:

- The effect of the treatments on fruit ethylene production has not been demonstrated in this study, ethylene production measurements should have been done to prove that the respiratory burst is linked to an increased ethylene production at day 4 and to demonstrate that 1-MCP treatment is blocking this ethylene burst.

I agree with the comment, but although we did not measure ethylene emission, in the 'Hayward' case, in previous studies such as Ilina et al. (2010), the respiratory burst is linked to an ethylene increase. However, despite we should have taken into account the ethylene rate measurement, the results show gene expression differences on ripening or ethylene-related genes. In further analysis of kiwifruit or other climactic fruits the ethylene emission will be considered.

- Some enzymes activity (involved in the glycolysis for example) could have been measured to confirm that the transcriptional regulation is effectively affecting the metabolism.

In the gene validation by RT-qPCR (Fig.10) is included the gene Achn219321 linked to PDC2 protein being this protein involved in the glycolysis. Anyway, in order to clarify the metabolic pathway of each gene, I've added the linked pathway between parenthesis.

- The last reference of the result part is wrong, the publication referenced is about MCP-1 for Monocyte chemoattractant protein-1 (Kim et al., 2014), the authors should be more careful.

Ok, this reference was eliminated because it was generating some confusion

The writing and organization of the manuscript could be improved:

- I suggest to call the three different treatments differently, calling them T0, T1 and T2 is confusing. I would suggest to call them not treated, 1-MCP and Ethrel® treatment instead.

As you have suggested T0, T1 and T2 were replaced by not treated, 1-MCP and Ethrel® treatments respectively throughout the manuscript.

- Why 48h after harvest is called day 1 and not day 2?

We consider to evaluate the fruit after 48 hours to facilitate the healing of the peduncular zone of the fruit, considering day 1 after 48h

- The last paragraph of the results is a discussion, it should be removed from the result part.

The last paragraph referred to gene validation (section: Confirming genes' expression using RT-qPCR) was modified, and some information in the discussion section was included (lines: 567-571).

- The title of the manuscript is unclear, I suggest "Transcriptome analysis and postharvest behavior of the kiwifruit 'Actinidia deliciosa' reveal the role of ethylene during fruit ripening" or similar.

The title was replaced by: "Transcriptome analysis and postharvest behavior of the kiwifruit 'Actinidia deliciosa' reveal the role of ethylene-related phytohormones during fruit ripening"

Several modifications of the formatting of the figures could greatly improved the reading of the manuscript:

- The color code should be mentioned on each figure and be more consistent between figures.

The color code or the description of each treatment and day is described in the legends

- I suggest to keep the same formatting in main and supplemental figure, for example keeping the color code red, blue purple in Supp. Fig1.

The formatting of Supp. Fig 1. has been remained because a color change in the color code does not favor the aesthetics of the figure. The rest of the figures were modified as suggested by the reviewer.

- Figure 3.

- o Top right panel: the blue color is not the same
- o Bottom panel: y-axis should start at 0

Blue color and y-axis have been modified in Fig. 3

- Figure 5 and 6 could be combined

Figures 5 and 6 were combined as Fig. 5.

- Figure 10. I suggest to go from White (min) to Red (max).

FPKM range was changed from White (min) to Red (max) and figures has been renamed to Figure 9

- Figure 11.

- o I suggest to use the same color code as in figure 1 (blue, red and purple)
- o The correspondence of the green to red colors is not clearly explained in the figure legend.

Figure 11 has been renamed to Figure 10 and I have replaced color code as in figure 1 (blue, red and purple) and raw Z-score were not considered in this figure.

Several mistakes and misformulations should be corrected, I suggest to the author to do a careful proofreading of the main text.

All of mistakes and misformulations were corrected after a detailed reading